PERGAMON

International Journal of Solids and Structures 37 (2000) 5413–5445

INTERNATIONAL JOURNAL OF SOLIDS and STRUCTURES

www.elsevier.com/locate/ijsolstr

Simulation of damped vibrations based on augmented Hooke's law and elastic modes of vibration

K. Dovstam

The Aeronautical Research Institute of Sweden, P.O. Box 11021, SE-161 11 Bromma, Sweden

Received 26 April 1998; in revised form 25 August 1999

Abstract

A linear, unconditionally convergent modal vibration response modelling technique is presented. Material damping is simulated using the augmented Hooke's law introduced by Dovstam [Dovstam, K., 1995. Augmented Hooke's law in frequency domain. A three-dimensional, material damping formulation. International Journal of Solids and Structures 32, 2835–2852]. The method is based on continuous, elastic, displacement modes and vibrational stress modes, dual to the traditional displacement modes. The stress modes are implicitly used to derive a generally convergent modal response model in generally damped cases with boundary traction excitation. The real eigenvalue problem defining the stress modes is formulated, and explicit frequency domain modal system equations of motion, for computation of needed stress and displacement mode coefficient spectra, are derived. Introduced parameters, accounting for the interdependence of the different modal contributions (modal coupling) to the response, are computable from known material properties (elastic and damping) and geometry by post processing results from three-dimensional, standard finite element (FE), eigenvalue calculations. Practical means for predicting whether modal coupling will occur or not are thus provided, as well as means for predicting damped resonance frequencies. When applied to an isotropic material, the new response model, for small damping, approaches the modal receptance model recently introduced and discussed by Dovstam [Dovstam, K., 1997. Receptance model based on isotropic damping functions and elastic displacement modes. International Journal of Solids and Structures 34, 2733–2754]. A close agreement between direct FE calculations and response simulations using the proposed method is obtained for a highly damped three-dimensional cantilever test plate.

Keywords: Damping; Vibrations; Elastic modes; Constitutive modelling; Augmented Hooke's law

1. Introduction

Despite the explosive development in computational power over the last 20 years, it is still prohibitively time consuming to compute vibration responses using detailed finite element (FE) models and direct frequency by frequency matrix inversion. This is especially true in analysis commonly

0020-7683/00/$ - see front matter
PII: S0020-7683(99)00237-1

encountered in vibroacoustical design problems. When available, the use of modal methods, therefore, provides a tremendous reduction of computation time for computations over wide frequency bands.

In general, vibrational modes in real physical systems are coupled in the sense that the corresponding mode coefficients are interdependent, and consequently, not easily computable directly from explicit formulae. As a result, general damped vibration responses have hitherto not been possible to analyse using generally convergent modal methods. The objective behind the work presented in this paper has, therefore, been to derive a modal method for simulation and prediction of generally damped linear vibrations.

The starting point of the present paper is the modal vibration response model, producing good approximations for cases having small but otherwise general damping and weakly interdependent mode coefficients, recently introduced by the author, Dovstam (1997). The present method resolves the inherent convergence problems associated with computation of strains by termwise differentiation of modal displacement series. It is shown that the noted convergence problems may be avoided by introduction of continuous stress modes, which are dual to the displacement modes. The concept of continuous, dual mode fields and their properties have, to the knowledge of the author, not until now been discussed and used in the literature.

The proposed method is based on the augmented Hooke's law (AHL) (Dovstam, 1995) and on the crucial observation that dual stress modes only implicitly have to be used in computation of responses for boundary traction excitation. The new method is convergent also in cases with very high damping and highly interdependent (coupled) mode coefficients. A benefit of the approach is that means for predicting whether mode coupling do occur are provided.

The proposed modal response model allows an explicit separation of elastic and geometry dependent modal properties from the dissipation and damping properties of vibrating continuous solids and structures. This is of great importance in experimental, indirect damping estimation based on measured responses, as discussed by Dovstam (1997), Dovstam and Dalenbring (1997) and Dalenbring (1999).

The main contributions of the present paper are:

1. an unconditionally convergent method for modal expansion of vibrational displacement fields in linear generally damped bodies and structures subjected to specified excitation forces (tractions) on the boundary,
2. formulation of the real eigenvalue problem for continuous, elastic, stress modes, dual to classical, continuous, displacement modes used in traditional modal expansion,
3. explicit frequency domain modal equations of motion for computation of approximations of the correct generalised Fourier coefficient functionals (stress and displacement mode coefficient spectra) in the case of excitation defined by forces on the boundary,
4. introduction of modal coupling parameters computable from given constitutive material properties (elastic and damping) and geometry by post processing results from three-dimensional FE approximation and standard eigenvalue calculations and
5. a novel theory for modal expansion of damped vibrational stress and strain fields based on continuous elastic stress modes.

The new method is verified on numerical test cases, which in a previously reported analysis (Dovstam, 1997) showed poor or very bad convergence for an uncoupled modal response model. The agreement between direct FE calculations and simulations using the new method is extremely good.

The paper starts with a brief discussion on localised boundary forces and corresponding receptance spectra. Following this, the governing linearised continuum mechanical equations of motion are presented. Elastic modes and mode series expansion of both displacements and stresses are then discussed. Finally, the new modal response model and the specific numerical test cases are presented.

Throughout the text, the Laplace transform, with respect to the time variable t, of a field or function

is denoted by a tilde above the particular parameter. The complex Laplace (frequency) variable is denoted by s and interpreted as $s = \alpha + i\omega$, where $\omega = 2\pi f$ is the current circular frequency in rad/s, while f is the vibration frequency in Hz. The current spatial point is denoted by $\mathbf{x}$, and the studied vibrating body is assumed to occupy a three-dimensional volume Ω with boundary $\partial\Omega$ in three-dimensional space. The mass density field of the body is $\rho = \rho(\mathbf{x})$. If not defined directly in the text, notations used may be found in Appendix A (Definitions) and Appendix B (Inner products and L_2 convergence).

2. Vibration response due to boundary forces

The transformed frequency domain displacement field $\tilde{\mathbf{u}}$ in a vibrating body can always be approximated using a modal expansion

$$\tilde{\mathbf{u}} \approx \sum_{m=1}^{N} c_m(\tilde{\mathbf{u}})\mathbf{w}^{(m)}(\mathbf{x}) \tag{1}$$

once the mode shapes $\mathbf{w}^{(m)}(\mathbf{x})$ and mode coefficients $c_m(\tilde{\mathbf{u}})$, $m = 1, 2, 3, \ldots, N$ have been computed (Dovstam, 1997, 1998a, 1998b). Generally, the mode coefficients are mutually interdependent and in such cases the modal contributions, i.e. the different terms in Eq. (1), are said to be coupled. It should be noted then, for linear vibrations, that coefficient spectra $c_m(\tilde{\mathbf{u}}) = c_m^{\mathrm{F}}(\tilde{\mathbf{u}})$ corresponding to a vibration field $\tilde{\mathbf{u}}$ caused by a specific excitation $\mathbf{F} = \alpha \cdot \mathbf{F}_a + \beta \cdot \mathbf{F}_b$, where α and β are complex numbers, depend linearly on $\mathbf{F}$ and thus $c_m^{\mathrm{F}}(\tilde{\mathbf{u}}) = \alpha \cdot c_m^{\mathrm{F}_a}(\tilde{\mathbf{u}}) + \beta \cdot c_m^{\mathrm{F}_b}(\tilde{\mathbf{u}})$.

The key issue, which is the main objective of the present paper, is to compute the mode coefficients $c_m(\tilde{\mathbf{u}})$, for linear but generally damped vibrations, when given as input the material properties (elastic and damping), the geometry and the excitation forces.

Cases of special interest are typically when the body is excited by a localised three-dimensional dynamic force $\mathbf{F}(t)$ distributed over a small part $\partial_{\mathrm{e}}\Omega$ of the boundary $\partial\Omega$. In such cases, which are common in vibroacoustics, the vibrational displacement responses are described by receptances, which are defined as the ratio of a displacement component spectrum $\tilde{u}_i(\mathbf{x}, s)$ and the complex amplitude $\tilde{F}(s) = \tilde{F}(\mathbf{x}_e, s) \equiv \tilde{\mathbf{F}}(s)/|\tilde{\mathbf{F}}(s)|$ of the excitation force spectrum $\tilde{\mathbf{F}}(s)$. The receptance R_{iF} corresponding to the force spectrum $\tilde{\mathbf{F}}$ at a point $\mathbf{x}_e$ on the boundary is thus defined as:

$$R_{iF} = R_{iF}(\mathbf{x}, \mathbf{x}_e, s) = \frac{\tilde{u}_i(\mathbf{x}, s)}{\tilde{F}(\mathbf{x}_e, s)} \tag{2}$$

and according to Eq. (1):

$$R_{iF} \approx \sum_{m=1}^{N} w_i^{(m)}(\mathbf{x}) \cdot c_m^{\mathrm{F}}(\tilde{\mathbf{u}})/\tilde{F} \tag{3}$$

Due to the interdependence between the mode coefficients, it is in general not possible to write down a simple explicit expression for the relation between each single mode coefficient spectrum $c_m(\tilde{\mathbf{u}})$ and the excitation $\tilde{\mathbf{F}}$. Therefore, $c_m(\tilde{\mathbf{u}})$ and $c_m^{\mathrm{F}}(\tilde{\mathbf{u}})/\tilde{F}$ have to be computed as solutions to a novel system of coupled modal equations of motion as will be shown below.

3. Governing equations in frequency domain

3.1. Equations of motion

Assuming zero body forces and zero initial conditions for the displacement field $\mathbf{u} = \mathbf{u}(\mathbf{x}, t)$ and the corresponding velocity field $\dot{\mathbf{u}} = \dot{\mathbf{u}}(\mathbf{x}, t)$, Laplace transformation of the linearised continuum mechanical equations of motion yields the following matrix equation:

$$-\mathbf{D}^{\mathrm{T}}[\tilde{\mathbf{T}}] + s^2\rho\tilde{\mathbf{u}} = \mathbf{0} \quad \mathbf{x} \in \Omega \tag{4}$$

for a continuum occupying the volume Ω in three-dimensional space at isothermal conditions.

The stresses $\mathbf{T}$ are defined according to the frequency domain AHL (Dovstam, 1995; 1999) as:

$$\tilde{\mathbf{T}} = \hat{\mathbf{H}}\tilde{\mathbf{E}} \quad \mathbf{x} \in \bar{\Omega} = \Omega \cup \partial\Omega \tag{5}$$

where the constitutive, material matrix field $\hat{\mathbf{H}}$ is defined by its elastic, zero frequency part $\mathbf{H}$ and the augmenting, complex and frequency dependent, anelastic part $\mathbf{H}_\Delta$ as:

$$\hat{\mathbf{H}} = \mathbf{H}(\mathbf{x}) + \mathbf{H}_\Delta(\mathbf{x}, s) \tag{6}$$

The inverse AHL

$$\tilde{\mathbf{E}} = \hat{\mathbf{C}}\tilde{\mathbf{T}} \tag{7}$$

is defined by the complex, inverse (compliance) material matrix field

$$\hat{\mathbf{C}} = \hat{\mathbf{H}}^{-1} = \left[\hat{\mathbf{H}}(\mathbf{x}, s)\right]^{-1} \tag{8}$$

and in analogy with Eq. (6) the augmenting, anelastic part of the inverse law is defined as:

$$\mathbf{C}_\Delta = \hat{\mathbf{C}} - \mathbf{C} \tag{9}$$

Here, $\mathbf{C}$ is the elastic, inverse Hooke's material matrix field:

$$\mathbf{C} = \mathbf{H}^{-1} = \left[\mathbf{H}(\mathbf{x})\right]^{-1} \tag{10}$$

Introducing Eq. (5) into the equation of motion, (4), leads to:

$$\hat{\mathbf{L}}[\tilde{\mathbf{u}}] + s^2\rho\tilde{\mathbf{u}} = \mathbf{0} \quad x \in \Omega \tag{11}$$

The frequency dependent, second order, spatial differential operator matrix $\hat{\mathbf{L}}$ is defined as:

$$\hat{\mathbf{L}}[\mathbf{v}] = -\mathbf{D}^{\mathrm{T}}[\hat{\mathbf{H}}\mathbf{D}[\mathbf{v}]] \quad \mathbf{x} \in \Omega \tag{12}$$

for smooth enough three-dimensional, complex vector fields $\mathbf{v}$. The domain of definition of the operator $\hat{\mathbf{L}}$ is important and depends on the boundary conditions imposed on the fields in the function space of which $\mathbf{v}$ is assumed to be a member of.

The boundary conditions for $\tilde{\mathbf{u}}$ are assumed to be mixed displacement and traction conditions:

$$\tilde{\mathbf{u}} = \hat{\mathbf{u}} \quad \mathbf{x} \in \partial_{\mathrm{u}}\Omega \tag{13}$$

$$\tilde{\mathbf{t}}_n = \mathbf{N}\hat{\mathbf{H}}\mathbf{D}[\tilde{\mathbf{u}}] = \hat{\mathbf{t}} \quad \mathbf{x} \in \partial_t\Omega = \partial\Omega - \partial_u\Omega \tag{14}$$

where $\hat{\mathbf{u}} = \hat{\mathbf{u}}(\mathbf{x}, s)$ and $\hat{\mathbf{t}} = \hat{\mathbf{t}}(\mathbf{x}, s)$ are frequency and position dependent, three-dimensional vector functions, specified on the boundary $\partial\Omega = \partial_u\Omega \cup \partial_t\Omega$. For free bodies, not fixed in space, the point set $\partial_u\Omega$ may be empty.

After operation with the strain operator $\mathbf{D}$ on Eq. (4) divided by ρ, and using the constitutive relation (7), the partial differential equation for the transformed, six-dimensional, stress field $\tilde{\mathbf{T}}$ is obtained as:

$$\mathbf{Q}\big[\tilde{\mathbf{T}}\big] + s^2\hat{\mathbf{C}}\tilde{\mathbf{T}} = \mathbf{0} \quad \mathbf{x} \in \Omega \tag{15}$$

where, for smooth enough six-dimensional complex vector fields $\mathbf{V}$, the second order, spatial differential operator matrix field $\mathbf{Q}$ is defined as:

$$\mathbf{Q}[\mathbf{V}] = -\mathbf{D}\big[\rho^{-1}\mathbf{D}^{\mathrm{T}}[\mathbf{V}]\big] \quad \mathbf{x} \in \Omega \tag{16}$$

A time domain, elastic counterpart to Eq. (15) was formulated by Ignaczak (1963), and it is worth noting that Eq. (15) expresses the pure stress formulation of the linearised equations of motion represented by Eqs. (4), (5), (7) and (11).

The differential operator $\mathbf{Q}$, in contrast to $\hat{\mathbf{L}}$, is self adjoint, irrespective of the material properties of the studied body. For details concerning domains (suitable function spaces including boundary conditions for $\tilde{\mathbf{u}}$ and $\tilde{\mathbf{T}}$) of partial differential operators, such as $\hat{\mathbf{L}}$ and $\mathbf{Q}$, the reader is referred to, e.g., Oden (1979) or Reddy (1986).

Boundary conditions for $\tilde{\mathbf{T}}$, equivalent to the conditions (13) and (14), are defined by the mixed conditions (natural and essential, respectively, for $\tilde{\mathbf{T}}$):

$$\mathbf{D}^{\mathrm{T}}\big[\tilde{\mathbf{T}}\big] = s^2\rho\hat{\mathbf{u}}, \quad \mathbf{x} \in \partial_u\Omega \tag{17}$$

$$\tilde{\mathbf{t}}_n \equiv \mathbf{N}\tilde{\mathbf{T}} = \hat{\mathbf{t}}, \quad \mathbf{x} \in \partial_t\Omega = \partial\Omega - \partial_u\Omega \tag{18}$$

It should be noted that the essential condition (13) imposed on the displacements $\tilde{\mathbf{u}}$ is equivalent to a natural condition on the stresses $\tilde{\mathbf{T}}$. Likewise the natural condition (14) for $\tilde{\mathbf{u}}$ is equivalent to an essential condition on the stresses $\tilde{\mathbf{T}}$. This is of importance in modal series expansion of $\tilde{\mathbf{u}}$ and $\tilde{\mathbf{T}}$, as essential boundary conditions require special attention, if the modal expansions should be convergent in a way useful for simulation of vibration responses.

3.2. Isotropic material properties

The constitutive matrix $\mathbf{H}$ of the isotropic, generalised Hooke's law may be written (Appendix A) as:

$$\mathbf{H} = G\mathbf{H}_G + \lambda\mathbf{H}_\lambda \tag{19}$$

and the corresponding isotropic, AHL is given by:

$$\hat{\mathbf{H}} = G\big(1 + d_G(s)\big)\mathbf{H}_G + \lambda\big(1 + d_\lambda(s)\big)\mathbf{H}_\lambda \tag{20}$$

where $d_G(s)$ and $d_\lambda(s)$ are damping functions (Dovstam, 1997) corresponding to the elastic Lamé's moduli G (shear modulus) and λ. The damping functions are material properties and vanish at zero frequency. The augmenting parts $Gd_G(s)$ and $\lambda d_\lambda(s)$ are completely independent of the elastic zero frequency properties and thus related to dissipation and material damping only. Details and alternative

damping function models may be found in Dovstam (1995, 1997, 1999) and Dovstam and Dalenbring (1997).

4. Elastic modes and mode series expansion

4.1. Introduction

The modal response model presented in Dovstam (1997) was based on Gurtins general results (Gurtin, 1972) concerning elastic displacement modes (classical, continuous, real normal modes) and their completeness in $\mathbf{L}_2^3(\Omega)$ (Appendix B). The pertinent theoretical background, summarised in Dovstam (1997, 1998a, 1998b), is also given here for reference purposes. Further, and more detailed, discussions of completeness and $L_2(\Omega)$ convergence may be found in Mikhlin (1964) and Oden (1979).

Continuous, elastic, stress modes and corresponding stress mode series are defined in Section 4.3. It is shown in Appendix C that the new type of stress mode series converges in $\mathbf{L}_2^6(\Omega)$ (Appendix B) due to the completeness in $\mathbf{L}_2^3(\Omega)$ of the displacement modes.

In the following, only the mixed boundary condition case with zero (essential) conditions on $\tilde{\mathbf{u}}$ ($\hat{\mathbf{u}} = \mathbf{0}$ in Eq. (13)) and the special case with pure traction (natural) boundary conditions for the displacement field $\tilde{\mathbf{u}}$ ($\partial_u\Omega$ empty in Eqs. (13) and (14)) will be discussed.

Non-zero displacement boundary conditions and modal expansions suitable for such cases are not included here, but will be discussed by the author in a forthcoming paper.

4.2. Displacement mode series

As already mentioned above, the Laplace transformed displacement field $\tilde{\mathbf{u}}$ in a vibrating body may, due to the completeness of the modes $\{\mathbf{w}^{(m)}\}_{m=1}^{\infty}$, always be represented by a generalised Fourier series and expressed as:

$$\tilde{\mathbf{u}}(\mathbf{x}, s) = \tilde{\mathbf{u}}_N(\mathbf{x}, s) + \tilde{\mathbf{u}}_{res}(\mathbf{x}, s) \quad \mathbf{x} \in \Omega \tag{21}$$

$$\tilde{\mathbf{u}}_N(\mathbf{x}, s) \equiv \sum_{m=1}^{N} c_m(\tilde{\mathbf{u}})\mathbf{w}^{(m)}(\mathbf{x}) \quad \mathbf{x} \in \Omega \tag{22}$$

where $\tilde{\mathbf{u}}_{res}(\mathbf{x}, s) = \tilde{\mathbf{u}}(\mathbf{x}, s) - \tilde{\mathbf{u}}_N(\mathbf{x}, s)$ is the point wise error of the (truncated series) approximation $\tilde{\mathbf{u}}_N$. The three-dimensional vector fields $\mathbf{w}^{(m)}$ are traditionally identified as undamped, elastic, natural (normal) modes of vibration and $\tilde{\mathbf{u}}_N$ is said to be a modal expansion corresponding to those modes. The modes are thus real, i.e., all component fields $w_k^{(m)} = w_k^{(m)}(\mathbf{x})$ are real valued. The s-dependent coefficients $c_m(\tilde{\mathbf{u}})$ are complex valued linear functionals of the Laplace transformed displacement field $\tilde{\mathbf{u}}$:

$$c_m(\tilde{\mathbf{u}}) = \left(\tilde{\mathbf{u}}, \rho\mathbf{w}^{(m)}\right)/a_m \quad m = 1, 2, \ldots \tag{23}$$

$$a_m = \left(\mathbf{w}^{(m)}, \rho\mathbf{w}^{(m)}\right) > 0 \quad m = 1, 2, \ldots \tag{24}$$

where $(\mathbf{u}, \mathbf{v})$ denotes the inner product in the function space $\mathbf{L}_2^3(\Omega)$ (Appendix B). Finally, the modes $\mathbf{w}^{(m)}$ are orthogonal (mass orthogonal) in the sense that (δ_{mr} is the Kronecker delta):

$$\left(\mathbf{w}^{(m)}, \rho\mathbf{w}^{(r)}\right) = a_m\delta_{mr} \quad m, r = 1, 2, \ldots \tag{25}$$

The fundamental problem in derivation of response models based on modal expansion is to explicitly calculate and predict the modal coefficients $c_m(\tilde{\mathbf{u}})$ corresponding to a given vibrational excitation. Generally, the different modal contributions $c_m(\tilde{\mathbf{u}})\mathbf{w}^{(m)}(\mathbf{x})$ in Eq. (22) are interdependent due to vibration damping, here represented by the anelastic material matrix $\mathbf{H}_\Delta$ in Eq. (6). This is commonly referred to as *coupling* or *modal coupling* which here is used synonymously to denote *interdependence between the modal coefficients* $c_m(\tilde{\mathbf{u}})$. Note that this form of coupling should not be confused with lack of orthogonality of the mode shapes $\mathbf{w}^{(m)}$ which are always mass-orthogonal as expressed by Eq. (25).

Certain boundary conditions are assumed to be satisfied by the modes, such that for all modal indices r and m

$$\left(\mathbf{NHE}^{(r)}, \mathbf{w}^{(m)}\right)_\partial = 0 \tag{26}$$

where $\mathbf{E}^{(r)} = \mathbf{D}[\mathbf{w}^{(r)}]$. The case of special interest here, in connection to the mixed conditions (13) and (14) on $\tilde{\mathbf{u}}$, is the *homogeneous, mixed conditions*:

$$\mathbf{w}^{(m)} = \mathbf{0} \quad \mathbf{x} \in \partial_{\mathrm{u}}\Omega \tag{27}$$

$$\mathbf{t}_{\mathrm{n}}^{(m)} \equiv \mathbf{NHD}\left[\mathbf{w}^{(m)}\right] = \mathbf{0} \quad \mathbf{x} \in \partial_{\mathrm{t}}\Omega = \partial\Omega - \partial_{\mathrm{u}}\Omega \tag{28}$$

Using FE techniques, it is easy and straightforward to compute good approximations of the continuous mode fields $\mathbf{w}^{(m)}(\mathbf{x})$ when the geometry and the elastic zero frequency material properties $\mathbf{H}$ of the body are known. However, in general, there exists no explicit formula for computation of the coefficients $c_m(\tilde{\mathbf{u}})$, unless the entire field $\tilde{\mathbf{u}}(\mathbf{x}, s)$ is known and, in which case, the definition (23) could be used, cf. Dovstam, 1997. In cases where unknown responses should be predicted an alternative to the definition (23) is thus needed.

Take the inner product of the equation of motion (11) and $\mathbf{w}^{(m)}$ and integrate the result by parts using Eq. (B8) given in Appendix B. Then, introducing the constitutive material field (6), using the definition (23) and homogeneous boundary conditions (13) for $\tilde{\mathbf{u}}$, non-zero traction conditions (14) and the conditions (27) and (28) for the modes, it is obtained that:

$$a_m\left[s^2 + \omega_m^2\right]c_m(\tilde{\mathbf{u}}) + \langle \mathbf{H}_\Delta\tilde{\mathbf{E}}, \mathbf{E}^{(m)}\rangle = \tilde{F}_\partial^{(m)} \tag{29}$$

which is the non-homogeneous and anisotropic, counterpart to Eq. (25) in Dovstam (1997). The complex function $\tilde{F}_\partial^{(m)}$ is the modal force spectrum which for generally distributed dynamic boundary forces is defined by a surface integral (Appendix B):

$$\tilde{F}_\partial^{(m)} = \left(\tilde{\mathbf{t}}_{\mathrm{n}}, \mathbf{w}^{(m)}\right)_\partial = \int_{\partial\Omega} \tilde{\mathbf{t}}_{\mathrm{n}} \cdot \mathbf{w}^{(m)}\, \mathrm{d}\partial\Omega \tag{30}$$

where $\mathbf{t}_{\mathrm{n}}$ is the time domain traction field defined by the external forces.

Eq. (29) points out the need of a generally convergent modal expansion of the inner product $\langle \mathbf{H}_\Delta\tilde{\mathbf{E}}, \mathbf{E}^{(m)}\rangle$. In traditional modal analysis, the strain $\tilde{\mathbf{E}}$ is usually approximated using term by term differentiation of a truncated modal expansion, corresponding to Eq. (22), assuming that $\tilde{\mathbf{E}} = D[\tilde{\mathbf{u}}] \approx \sum_{m=1}^{N} c_m(\tilde{\mathbf{u}})\mathbf{E}^{(m)}$. However, it turns out, as will be shown later, that a correct modal expansion of the strain field $\tilde{\mathbf{E}}$ does not have the same Fourier coefficients $c_m(\tilde{\mathbf{u}})$ as the displacement field $\tilde{\mathbf{u}}$, and that the strain fields $\mathbf{E}^{(m)}$ do not constitute a proper basis for $\tilde{\mathbf{E}}$ in the function space $\mathbf{L}_2^6(\Omega)$ (Appendix B).

Derivation of the generalised Fourier coefficients $c_m(\tilde{\mathbf{u}})$ for the displacement response $\tilde{\mathbf{u}}$ may start from the equation of motion, (11), or from the "elastic" partial differential equation (no sum on m):

$$\mathbf{L}\left[\mathbf{w}^{(m)}\right] - \omega_m^2 \cdot \rho \mathbf{w}^{(m)} = \mathbf{0} \quad \mathbf{x} \in \Omega \tag{31}$$

defining the modes $\mathbf{w}^{(m)}$, which constitute a *set of complete* (Gurtin, 1972) *basis vector fields* in the function space $\mathbf{L}_2^3(\Omega)$ (Appendix B). Here, the "elastic", second order, differential operator $\mathbf{L}$ is defined by the elastic material matrix field $\mathbf{H} = \mathbf{H}(\mathbf{x})$ as:

$$\mathbf{L}[\mathbf{w}] = -\mathbf{D}^{\mathrm{T}}[\mathbf{H}\mathbf{D}[\mathbf{w}]] \quad \mathbf{x} \in \Omega \tag{32}$$

4.3. Stress mode series

The stress field $\tilde{\mathbf{T}}$ in a vibrating body can, as shown in Appendix C, be represented by a generalised Fourier series, convergent in $\mathbf{L}_2^6(\Omega)$, as:

$$\tilde{\mathbf{T}} \approx \tilde{\mathbf{T}}_N \equiv \sum_{m=1}^{N} g_m(\tilde{\mathbf{T}}) \mathbf{S}^{(m)}(\mathbf{x}) \tag{33}$$

where the vector fields $\mathbf{S}^{(m)}$ are six-dimensional real, elastic, stress modes. The frequency dependent coefficient functionals $g_m(\tilde{\mathbf{T}})$ may, in an analogous way as $c_m(\tilde{\mathbf{u}})$, be expressed as complex valued functionals depending on elastic (undamped) modal parameters (defined by the zero frequency elastic moduli and the geometry), the damping and the modal boundary conditions.

The generalised stress Fourier coefficients $g_m(\tilde{\mathbf{T}})$ are defined as:

$$g_m(\tilde{\mathbf{T}}) = \frac{\langle \tilde{\mathbf{T}}, \mathbf{C}\mathbf{S}^{(m)} \rangle}{L_m} \quad m = 1, 2, \ldots \tag{34}$$

$$L_m = \langle \mathbf{S}^{(m)}, \mathbf{C}\mathbf{S}^{(m)} \rangle \quad m = 1, 2, \ldots \tag{35}$$

The stress modes $\mathbf{S}^{(m)}$ satisfy, and are defined by, the "elastic" boundary value problem:

$$\mathbf{Q}\left[\mathbf{S}^{(m)}\right] - \bar{\omega}_m^2 \cdot \mathbf{C}\mathbf{S}^{(m)} = \mathbf{0} \tag{36}$$

$$\left(\rho^{-1}\mathbf{D}^{\mathrm{T}}\left[\mathbf{S}^{(m)}\right], \mathbf{N}\mathbf{S}^{(r)}\right)_{\partial} = 0 \quad \text{all } m, r \tag{37}$$

They satisfy the orthogonality conditions:

$$\langle \mathbf{S}^{(m)}, \mathbf{C}\mathbf{S}^{(r)} \rangle = L_m \cdot \delta_{mr} \quad \text{all } m, r \tag{38}$$

and are assumed to constitute a complete basis for the Hilbert space $\mathbf{L}_2^6(\Omega)$ (see Appendix B and the comment on convergence in Appendix C).

4.4. Dual stress and displacement modes

Both sets of modes $\mathbf{w}^{(m)}$, (22), and $\mathbf{S}^{(m)}$, (33), are "classical" in the sense that they are continuous and continuously differentiable as many times as needed. They may also be approximated, to any needed degree of accuracy, using FE modelling techniques. It is assumed here that the mode sets $\mathbf{w}^{(m)}$ and $\mathbf{S}^{(m)}$ correspond to the same elastic material and the same geometry and also to the same boundary partitions (sub-surfaces) $\partial_{\mathrm{u}}\Omega$ and $\partial_{\mathrm{t}}\Omega = \partial\Omega - \partial_{\mathrm{u}}\Omega$.

In the modal method proposed below, two *duality relations* between the displacement modes $\mathbf{w}^{(m)}$ and the stress modes $\mathbf{S}^{(m)}$ are crucial. Using Eqs. (31), (36), (16) and (32), together with spatial differentiation, it is always possible to write the duality relations as (Appendix D):

$$\mathbf{w}^{(m)} = -\omega_m^{-2}\rho^{-1}\mathbf{D}^{\mathrm{T}}\big[\mathbf{S}^{(m)}\big] \tag{39}$$

$$\mathbf{S}^{(m)} = \mathbf{H}\mathbf{E}^{(m)} = \mathbf{H}\mathbf{D}\big[\mathbf{w}^{(m)}\big] \tag{40}$$

and as a consequence of Eq. (26), it follows also that

$$\big(\mathbf{w}^{(m)}, \mathbf{N}\mathbf{S}^{(r)}\big)_{\partial} = 0 \tag{41}$$

for all indices r and m. Displacement modes $\mathbf{w}^{(m)}$ and stress modes $\mathbf{S}^{(m)}$ satisfying Eqs. (39)–(41) are here said to be *dual modes*.

The boundary conditions for the modes are further said to be *compatible with the displacements* $\tilde{\mathbf{u}}$ when the modes $\mathbf{w}^{(m)}$ satisfy the same homogeneous, displacement boundary conditions as $\tilde{\mathbf{u}}$ on $\partial_{\mathrm{u}}\Omega$. The $\tilde{\mathbf{u}}$-compatibility of the modes may be expressed as (noting that $\partial\Omega = \partial_{\mathrm{u}}\Omega \cup \partial_{\mathrm{t}}\Omega$):

$$\big(\tilde{\mathbf{u}}, \mathbf{t}_{\mathrm{n}}^{(m)}\big)_{\partial} = 0 \tag{42}$$

which is assumed to be fulfilled also in cases when $\partial_{\mathrm{u}}\Omega$ is empty. It should be noted then that

$$\mathbf{t}_{\mathrm{n}}^{(m)} = \mathbf{N}\mathbf{S}^{(m)} = \mathbf{N}\mathbf{H}\mathbf{E}^{(m)} = \mathbf{N}\mathbf{H}\mathbf{D}\big[\mathbf{w}^{(m)}\big] \tag{43}$$

for dual modes $\mathbf{S}^{(m)}$ and $\mathbf{w}^{(m)}$. The relationship $\mathbf{S}^{(m)} = \mathbf{H}\mathbf{E}^{(m)}$, (40), and partial integration further results in (cf. Eqs. (B9), (B10), (25), (31) and (32)):

$$\langle \mathbf{S}^{(m)}, \mathbf{C}\mathbf{S}^{(r)} \rangle = \langle \mathbf{S}^{(m)}, \mathbf{E}^{(r)} \rangle = \langle \mathbf{H}\mathbf{E}^{(m)}, \mathbf{E}^{(r)} \rangle = a_m \omega_m^2 \cdot \delta_{mr} \tag{44}$$

which should be compared to Eq. (38).

Taking the inner product of Eq. (11) and $\mathbf{w}^{(m)}$, integrating by parts using Eq. (B8) and using the definition (23), it is derived that (no sum on m):

$$\langle \hat{\mathbf{H}}\tilde{\mathbf{E}}, \mathbf{E}^{(m)} \rangle + s^2 a_m c_m(\tilde{\mathbf{u}}) = \big(\tilde{\mathbf{t}}_{\mathrm{n}}, \mathbf{w}^{(m)}\big)_{\partial} \tag{45}$$

Due to Eqs. (5), (34), (38), (44) and the duality $\mathbf{E}^{(m)} = \mathbf{C}\mathbf{S}^{(m)}$, Eq. (45) is equivalent to:

$$s^2 a_m c_m(\tilde{\mathbf{u}}) + a_m \cdot \omega_m^2 \cdot g_m(\tilde{\mathbf{T}}) = \tilde{F}_{\partial}^{(m)} \tag{46}$$

for dual, $\tilde{\mathbf{u}}$-compatible mode fields $\mathbf{w}^{(m)}$ and $\mathbf{S}^{(m)}$. The displacement coefficients $c_m(\tilde{\mathbf{u}})$ are thus directly related to, and computable from, the stress coefficients $g_m(\tilde{\mathbf{T}})$ and the modal forces $\tilde{F}_{\partial}^{(m)}$ defined by the vibrational surface tractions. Eq. (46) should be compared to Eq. (29) which in fact is equivalent to Eq. (46) for dual, $\tilde{\mathbf{u}}$-compatible modes.

It will be shown in the following that the stress mode coefficients $g_m(\tilde{\mathbf{T}})$ are generally interdependent. A consequence of this and Eq. (46) is that modal coupling defined as interdependence between the displacement coefficients $c_m(\tilde{\mathbf{u}})$ is *equivalent to* mutual interdependence of the stress mode coefficients.

5. Coupled mode coefficient functionals

5.1. Background

A crucial point in the present paper is the derivation of the stress coefficients $g_m(\tilde{\mathbf{T}})$. When the vibrational excitation is defined by *boundary tractions* alone, or combined with zero displacement conditions (part of the boundary fixed in space), it is possible to derive *modal system equations* which may be used *for approximation of the stress mode coefficients* $g_m(\tilde{\mathbf{T}})$ *without explicitly knowing the stress modes*. Once the $g_m(\tilde{\mathbf{T}})$ are known, the $c_m(\tilde{\mathbf{u}})$ may then be computed using Eq. (46).

5.2. Stress mode system equations

Substituting $\hat{\mathbf{H}}\tilde{\mathbf{E}}$ by $\tilde{\mathbf{T}}$ in Eq. (45), results in:

$$s^2 a_m c_m(\tilde{\mathbf{u}}) + \langle \tilde{\mathbf{T}}, \mathbf{E}^{(m)} \rangle = \tilde{F}_\partial^{(m)} \tag{47}$$

Unconstrained bodies, allowed to move freely in space due to the excitation, always have six ''rigid'', *zero frequency modes* with zero strain and, therefore, also zero stress. It thus follows from Eq. (47), with vanishing $\mathbf{E}^{(m)}$, that the corresponding mode coefficients are given directly and explicitly as $c_m(\tilde{\mathbf{u}}) = \tilde{F}_\partial^{(m)}/(a_m s^2)$.

Further, taking the inner product of Eq. (31) and $\tilde{\mathbf{u}}$ and integrating by parts, using Eqs. (32) and (B7), and applying the conditions (41), for $\tilde{\mathbf{u}}$-compatible modes:

$$\langle \mathbf{H}\tilde{\mathbf{E}}, \mathbf{E}^{(m)} \rangle = a_m \cdot \omega_m^2 \cdot c_m(\tilde{\mathbf{u}}) \tag{48}$$

Then, with $\tilde{\mathbf{E}} = \hat{\mathbf{C}}\tilde{\mathbf{T}}$ in Eq. (48), elimination of $c_m(\tilde{\mathbf{u}})$ using Eqs. (47) and (48) results in:

$$\omega_m^2 \cdot \langle \tilde{\mathbf{T}}, \mathbf{E}^{(m)} \rangle + s^2 \cdot \langle \mathbf{H}\hat{\mathbf{C}}\tilde{\mathbf{T}}, \mathbf{E}^{(m)} \rangle = \omega_m^2 \cdot \tilde{F}_\partial^{(m)} \tag{49}$$

To proceed, a relation between the coefficients $g_m(\tilde{\mathbf{T}})$ and the modal forces $\tilde{F}_\partial^{(m)}$ is required. After modal expansion of $\tilde{\mathbf{T}}$ in Eq. (49) using the definition (33) and utilising orthogonality properties (44) and the properties (41) and (42) of compatible modes and displacements, it is thus obtained for each $m = 1, 2, 3, \ldots$ (no sum on m):

$$a_m \omega_m^4 \cdot g_m(\tilde{\mathbf{T}}) + s^2 \cdot \sum_{r=1}^{\infty} \langle \mathbf{H}\hat{\mathbf{C}}\mathbf{H}\mathbf{E}^{(m)}, \mathbf{E}^{(r)} \rangle \cdot g_r(\tilde{\mathbf{T}}) = \omega_m^2 \cdot \tilde{F}_\partial^{(m)} \tag{50}$$

These relations define an infinite dimensional system of equations characterising the stress mode coupling, that is the interdependence between the stress mode coefficient functionals, caused by the anelasticity represented by $\mathbf{C}_\Delta = \hat{\mathbf{C}} - \mathbf{C}$.

It is noted here that Eq. (50) corresponds to an unconditionally convergent modal expansion of the inner product $\langle \mathbf{H}_\Delta \tilde{\mathbf{E}}, \mathbf{E}^{(m)} \rangle$ in Eq. (29). Also, the inner product $\langle \mathbf{H}_\Delta \tilde{\mathbf{E}}, \mathbf{E}^{(m)} \rangle$ may be expressed as $a_m \omega_m^2 (g_m(\tilde{\mathbf{T}}) - c_m(\tilde{\mathbf{u}}))$, showing that the coefficient functionals $g_m(\tilde{\mathbf{T}})$ and $c_m(\tilde{\mathbf{u}})$ are identical when the anelasticity is zero.

It is further observed that:

$$\mathbf{H}\hat{\mathbf{C}}\mathbf{H} = \mathbf{H} + \mathbf{H}\mathbf{C}_\Delta\mathbf{H} \tag{51}$$

which is used below to simplify the Eq. (50).

Because the *non-zero stress modes* only, i.e., modes with $\omega_m > 0$, are of interest here, it follows that due to Eqs. (50), (51) and (44) for those modes (no sum on m):

$$a_m \cdot \left(\omega_m^2 + s^2\right) \cdot g_m(\tilde{\mathbf{T}}) + \frac{s^2}{\omega_m^2} \cdot \sum_{r=1}^{\infty} \langle \mathbf{H}\mathbf{C}_\Delta \mathbf{H}\mathbf{E}^{(m)}, \mathbf{E}^{(r)} \rangle \cdot g_r(\tilde{\mathbf{T}}) = \tilde{F}_\partial^{(m)} \tag{52}$$

When written in (infinite) matrix form, this is equivalent to:

$$\begin{bmatrix} B_{11} & B_{12} & B_{13} & B_{14} & \cdot & \cdot & \cdot \\ B_{21} & B_{22} & \cdot & \cdot & \cdot & \cdot & \cdot \\ \cdot & \cdot & \cdot & \cdot & \cdot & \cdot & \cdot \\ \cdot & \cdot & \cdot & B_{mr} & \cdot & \cdot & \cdot \\ \cdot & \cdot & \cdot & \cdot & \cdot & \cdot & \cdot \end{bmatrix} \begin{bmatrix} g_1(\tilde{\mathbf{T}}) \\ g_2(\tilde{\mathbf{T}}) \\ \cdot \\ g_r(\tilde{\mathbf{T}}) \\ \cdot \end{bmatrix} = \begin{bmatrix} \tilde{F}_\partial^{(1)} \\ \tilde{F}_\partial^{(2)} \\ \cdot \\ \tilde{F}_\partial^{(m)} \\ \cdot \end{bmatrix} \tag{53}$$

where the *non-symmetric* system matrix elements B_{mr} are given by (no sum on m):

$$B_{mr} = \begin{cases} a_m \left[\omega_m^2 + s^2 \cdot \left\{ 1 + \dfrac{1}{a_m \omega_m^2} \cdot \langle \mathbf{H}\mathbf{C}_\Delta \mathbf{H}\mathbf{E}^{(m)}, \mathbf{E}^{(m)} \rangle \right\} \right], & r = m \\ \dfrac{s^2}{\omega_m^2} \cdot \langle \mathbf{H}\mathbf{C}_\Delta \mathbf{H}\mathbf{E}^{(m)}, \mathbf{E}^{(r)} \rangle, & r \neq m \end{cases} \tag{54}$$

The complex, frequency dependent, modal strain energy integrals $\langle \mathbf{H}\mathbf{C}_\Delta \mathbf{H}\mathbf{E}^{(m)}, \mathbf{E}^{(r)} \rangle$ determine *completely* the coupling between the stress modes and may be computed using FE techniques and *partial stiffness matrices* (cf. Dovstam, 1997). In applications of course only a finite, but large enough, number, N, of modes are used in the modal expansions Eqs. (22), (33) and (53) is approximated by the N "first" equations and modes only, m, $r = 1, 2, 3, \ldots, N$ (not counting the zero frequency, rigid, modes in the case of an unconstrained body).

Thus, the fundamental prediction problem, how to compute the coefficient functionals $c_m(\tilde{\mathbf{u}})$ in Eqs. (1) and (22) in generally damped cases, is satisfactorily answered by the Eqs. (53) and (54) combined with Eq. (46). Solving Eqs. (53) and (54) for the stress coefficients $g_m(\tilde{\mathbf{T}})$, allows for solution of the displacement coefficients $c_m(\tilde{\mathbf{u}})$ from Eq. (46) when the vibration excitation is given in terms of the boundary tractions $\tilde{\mathbf{t}}_n$ which define the modal forces $\tilde{F}_\partial^{(m)}$ according to Eq. (30).

From the discussion above, it should be clear that the modal expansion (33) of the current stress field $\tilde{\mathbf{T}}$ and the duality between the stress modes and displacement modes are necessary and crucial for derivation of the correct coefficient functionals $c_m(\tilde{\mathbf{u}})$.

5.3. Damped resonances and modal shift functions

In the special case of *fully isotropic properties*, i.e., isotropic elasticities and damping:

$$\mathbf{H}\mathbf{C}_\Delta \mathbf{H} = a \cdot G\mathbf{H}_G + b \cdot \lambda \mathbf{H}_\lambda \tag{55}$$

where the complex, frequency dependent and possibly also position dependent material functions $a = a(s)$ and $b = b(s)$ may be expressed in terms of the isotropic material damping functions $d_G(s)$ and $d_\lambda(s)$ (Section 3.2). It may be derived that:

$$a = -\frac{d_G(s)}{1 + d_G(s)} \tag{56}$$

$$b = -\frac{d_\lambda(s) + \frac{\left[d_G(s)\right]^2}{(1 + 3\lambda/2G)} + \frac{d_\lambda(s) \cdot d_G(s)}{(1 + 2G/3\lambda)}}{\left[1 + d_G(s)\right] \cdot \left[1 + \frac{d_G(s)}{(1 + 3\lambda/2G)} + \frac{d_\lambda(s)}{(1 + 2G/3\lambda)}\right]} \tag{57}$$

In the case of *fully isotropic* and *homogeneous* properties, finally (no sum on m):

$$B_{mr} = \begin{cases} a_m\left\{s^2 \cdot \left[1 + \delta_m(s)\right] + \omega_m^2\right\}, & r = m \\ s^2 \cdot c(s) \cdot \dfrac{\gamma_{mr}}{\omega_m^2}, & r \neq m \end{cases} \tag{58}$$

$$\delta_m(s) = \chi_m a(s) + \left(1 - \chi_m\right) b(s) \tag{59}$$

$$c(s) = a(s) - b(s) = \frac{d_\lambda(s) - d_G(s)}{\left[1 + d_G(s)\right] \cdot \left[1 + \frac{1 + d_G(s)}{1 + 3\lambda/2G} + \frac{d_\lambda(s)}{1 + 2G/3\lambda}\right]} \tag{60}$$

$$\gamma_{mr} = \langle G\mathbf{H}_G\mathbf{E}^{(m)}, \mathbf{E}^{(r)}\rangle = 2\int_\Omega G\varepsilon_{ik}^{(m)}\varepsilon_{ik}^{(r)}\,\mathrm{d}\Omega \quad \text{(sum on } i, k\text{)} \tag{61}$$

$$\chi_m = \frac{\gamma_{mm}}{a_m\omega_m^2} \quad \text{(no sum on } m\text{)} \tag{62}$$

Here, the parameters γ_{mr} are partial, isotropic, *elastic modal strain energies* corresponding to the isotropic shear modulus G. The parameters χ_m are isotropic modal *weight factors* which determine the contributions of the material functions $a = a(s)$ and $b = b(s)$ to the complex, mode dependent functions $\delta_m(s)$. It is interesting to note that, according to Eq. (62), the weights χ_m are defined by the undamped resonance frequencies ω_m and the diagonal terms of the partial strain energy matrix (γ_{mr}). Thus, it is obvious that the energies γ_{mr}, and also the weights χ_m, depend, indirectly, on geometry, the mass distribution, the elasticities and the (modal) boundary conditions. Therefore, all modal parameters ω_m, χ_m, γ_{mr} and $\delta_m(s)$ are *structural properties*, and the modal functions $\delta_m(s)$ are *different for different geometries* even if the corresponding bodies or structures have identical material properties. However, the functions $d_G(s)$, $d_\lambda(s)$, $a(s)$ and $b(s)$ are only related to the material.

FE *approximation* of modal weight factors χ_m and strain energies γ_{mr} was discussed by the author already in Dovstam (1997). In Dovstam (1997) though, these parameters were used in a different context, connected to the uncoupled modal receptance model discussed therein.

The ''damped'' circular resonance frequency ω_{md}, corresponding to the undamped frequency ω_m, is now defined as:

$$\omega_{md} = \frac{\omega_m}{\sqrt{1 + \mathrm{Re}\left[\delta_m(i\omega_{md})\right]}} \tag{63}$$

which is a natural definition when looked at the real part of the diagonal elements in Eq. (58). The damped resonance peak of the response contribution from mode number m is thus "shifted", by the damping, from the undamped circular frequency ω_m to the damped frequency ω_{md}. Due to this frequency shifting effect, the functions $\delta_m(s)$ are in the following denoted *modal shift functions*. As already mentioned above, the shift functions are *structural properties* and depend not only on the material damping alone. According to Eqs. (58) and (63), it is also clear that large modal frequency shifts may occur even if the modal coupling is small. In the general case, the modal shift functions are given by:

$$\delta_m(s) = \frac{1}{a_m \omega_m^2} \langle \mathbf{H}\mathbf{C}_\Delta \mathbf{H}\mathbf{E}^{(m)}, \mathbf{E}^{(m)} \rangle \quad \text{no sum on } m \tag{64}$$

Furthermore, at a resonance $s = i\omega_{md}$ are, according to Eqs. (63) and (58), the diagonal elements of the modal system matrix purely imaginary:

$$[B_{mm}]_{s=i\omega_{md}} = -i a_m \omega_{md}^2 \, \mathrm{Im}\big[\delta_m(i\omega_{md})\big] \quad \text{no sum on } m \tag{65}$$

In analogy to this, damped circular resonance frequencies in general anisotropic and non-homogeneous cases are defined as those frequencies where the diagonal elements in Eqs. (53) and (54) are purely imaginary.

5.4. Modal coupling

Traditionally, and also here, modal coupling is regarded as *interdependency* between the displacement mode coefficients $c_m(\tilde{\mathbf{u}})$ in the modal expansion (22). Based on the new theory presented above, it is possible, though, to establish a deeper understanding of the cause of modal coupling occurring for vibrating bodies with continuous properties.

Here the *isotropic* modal *coupling matrix* (C_{mr}) is defined as:

$$C_{mr} = \frac{\gamma_{mr}}{a_m \omega_m^2} \quad \text{no sum on } m \tag{66}$$

and the off-diagonal terms of this matrix determine, together with the material functions $a = a(s)$ and $b = b(s)$, according to Eqs. (58)–(60), completely the stress mode coupling in the case of fully isotropic and homogeneous material properties.

For *small stress mode coupling* (small off-diagonal modal system matrix elements $s^2 \cdot c(s) \cdot a_m \cdot C_{mr}$, $r \neq m$ and thus weak interdependence between the stress mode coefficients), it is possible to derive, from Eqs. (46), (53), (54), (58), the explicit expression (*no sum on m*):

$$c_m(\tilde{\mathbf{u}}) \approx \frac{\tilde{F}_\partial^{(m)}(s)}{a_m\big[s^2 + \omega_m^2/\big(1 + \delta_m(s)\big)\big]} \quad \textit{small} \text{ stress mode coupling} \tag{67}$$

for the displacement mode coefficient functional $c_m(\tilde{\mathbf{u}})$. It should be noted that the approximation (67) represents the correct way of neglecting modal coupling, correct also for arbitrarily high damping. Modal coupling is thus equivalent to coupling between the stress modes, i.e., to mutual interdependence between the stress mode coefficients $g_m(\tilde{\mathbf{T}})$ caused by the inelasticity $\mathbf{C}_\Delta$. Explicit expressions analogous to Eq. (67) but corresponding to more general cases (anisotropic, inhomogeneous but still continuous $\mathbf{H}$ and $\mathbf{C}_\Delta$) may be derived from Eqs. (46), (53) and (54), assuming that the off-diagonal system matrix elements $B_{mr}(s)$, $r \neq m$ may be neglected.

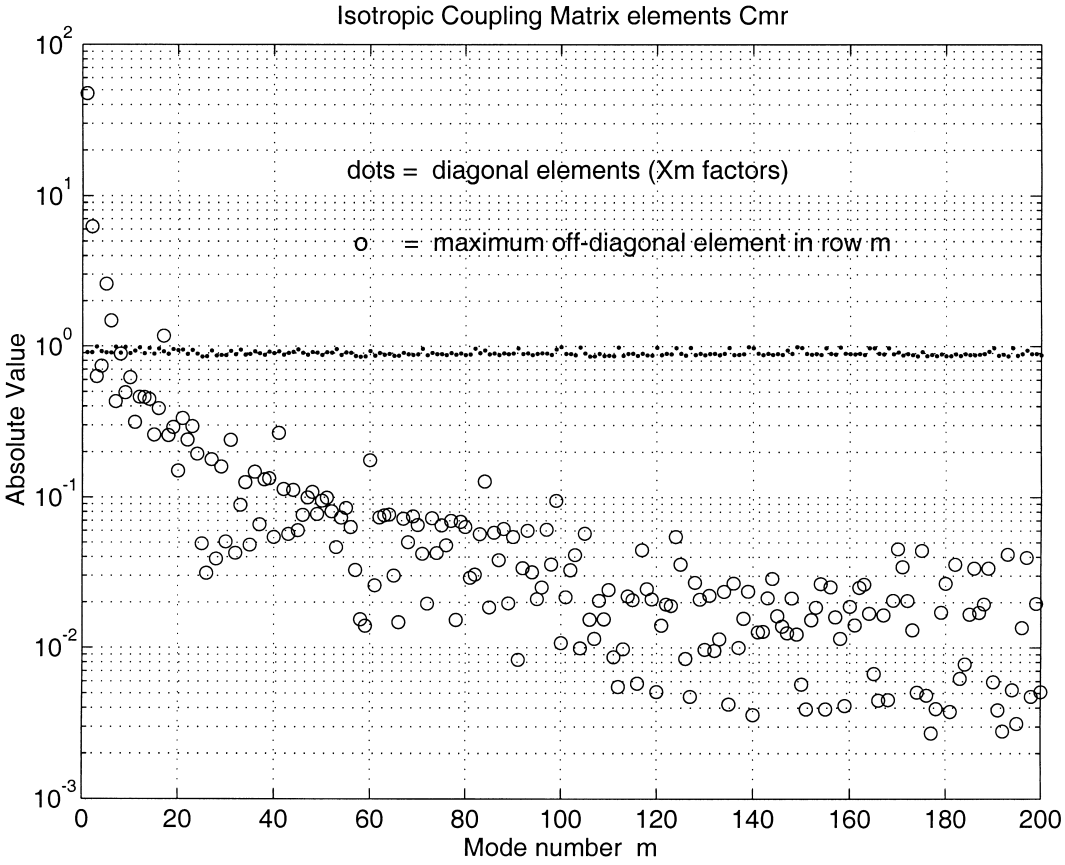

Fig. 1. Diagonal (.....) and maximum (○ ○ ○) coupling matrix elements C_{mr} for test plate.

In the general case, *when stress mode coupling may not be neglected*, the displacement coefficient functional $c_m(\tilde{\boldsymbol{u}})$, due to Eqs. (46) and (53), can be expressed as (no sum on m):

$$c_m(\tilde{\mathbf{u}}) = \frac{\left[1 - a_m\omega_m^2 I_{mm}(s)\right]}{a_m s^2} \cdot \tilde{F}_{\partial}^{(m)}(s) - \left(\frac{\omega_m}{s}\right)^2 \sum_{r\neq m} I_{mr}(s) \cdot \tilde{F}_{\partial}^{(r)}(s) \tag{68}$$

Table 1
AHL material damping parameters for the test plate

AHL parameters ($n = 1, 2, 3$)	Case A (Fig. 9, Dovstam, 1997)	Case B (Fig. 8, Dovstam, 1997)	Case C (new case, $d_{\lambda} = 0$)
$\beta_n/2\pi$ (Hz)	10, 100, 800	10, 100, 800	10, 150, 1000
φ_n (Pa)	$\varphi_1 = 18{,}974$; $\varphi_2 = 25{,}298$; $\varphi_3 = 37{,}947$	$\varphi_1 = 12{,}000$; $\varphi_2 = 16{,}000$; $\varphi_3 = 24{,}000$	$\varphi_1 = \varphi_2 = \varphi_3 = 0$
μ_n (Pa)	$\mu_1 = \mu_2 = \mu_3 = 750$	$\mu_1 = \mu_2 = \mu_3 = 7500$	$\mu_1 = 12{,}649$; $\mu_2 = 20{,}555$; $\mu_3 = 37{,}947$

Table 2
Elastic (undamped) frequencies $f_m = \omega_m/2\pi$, isotropic weight factors χ_m and modal frequency shift $\Delta_m = (f_{md} - f_m)/f_m$, predicted by Eq. (63), for modes with damped resonance frequency $f_{md} = \omega_{md}/2\pi$ below 700 Hz

Mode number, m	Elastic frequency, f_m (Hz)	Modal weight, χ_m	Δ_m, Case A (%)	Δ_m, Case B (%)	Δ_m, Case C (%)
1	3.96	0.91	0.90	0.90	5.95
2	24.8	0.91	2.35	7.18	19.3
3	53.4	0.99	0.33	7.82	34.8
4	67.5	0.92	2.20	9.90	36.9
5	69.6	0.91	2.92	10.1	36.6
6	136.7	0.90	3.47	12.8	55.3
7	162.0	0.99	0.48	11.5	72.4
8	226.6	0.90	3.90	14.5	69.8
9	275.8	0.99	0.66	12.8	93.3
10	339.3	0.90	4.32	15.8	83.1
11	389.3	0.93	2.86	15.2	
12	397.6	0.98	0.97	13.9	
13	475.0	0.89	4.72	17.1	
14	530.6	0.97	1.32	15.0	
15	633.3	0.89	5.07		
16	676.6	0.96	1.72		

where the complex functions $I_{mr}(s)$ denote the elements of the inverse $\mathbf{I}(s) = [\mathbf{B}(s)]^{-1}$ of the modal system matrix $\mathbf{B}(s)$ in Eq. (53). It is obvious that all *modal receptance* functions $-(\omega_m/s)^2 \cdot I_{mr}(s)$ with $r \neq m$ have to be small, compared to the factor $[1 - a_m\omega_m^2 \cdot I_{mr}(s)]/(a_{ms}^2)$ of the first term on the right-hand side of Eq. (68), to make it possible to neglect the modal coupling for mode number m. As expected, Eqs. (67) and (68) give identical results when the off-diagonal functions $-(\omega_m/s)^2 \cdot I_{mr}(s)$ are either zero or neglected.

The expression (67), and the appearance of the modal shift function $\delta_m(s)$, should be compared to the corresponding expression in Dovstam (1997) derived for uncoupled cases, i.e., cases with uncoupled mode coefficients. For *small damping*, i.e. small $|d_G(s)|$ and $|d_\lambda(s)|$, it may be shown that:

$$\frac{1}{(1+\delta_m)} \approx 1 - \delta_m + \delta_m^2 - \delta_m^3 + \cdots \approx 1 + d_m + O(|d_G^2|) + O(|d_\lambda^2|) \tag{69}$$

where $d_m = d_m(s)$ denotes the modal damping function introduced in Dovstam (1997). Thus, for *small stress mode coupling* combined with *small damping*, the new correctly coupled model and the old "uncoupled" model discussed in Dovstam (1997) correspond to *approximately the same displacement mode coefficients*. For *proportional damping*, i.e. when $d_G(s) = d_\lambda(s)$, the coefficients $c_m(\tilde{\mathbf{u}})$ of the new and the old uncoupled model turn out to be identical.

6. Numerical test case

6.1. Introduction

In order to test the new coupled modal receptance model, receptances R_{iF}, defined by the Eqs. (2), (3), (30), (46), (53) and (55)–(62), have been computed and compared to corresponding receptances calculated by *direct FE response analysis*, i.e., frequency by frequency inversion of the (complex and frequency dependent) global dynamic stiffness matrix of the FE model. The direct FE response analysis

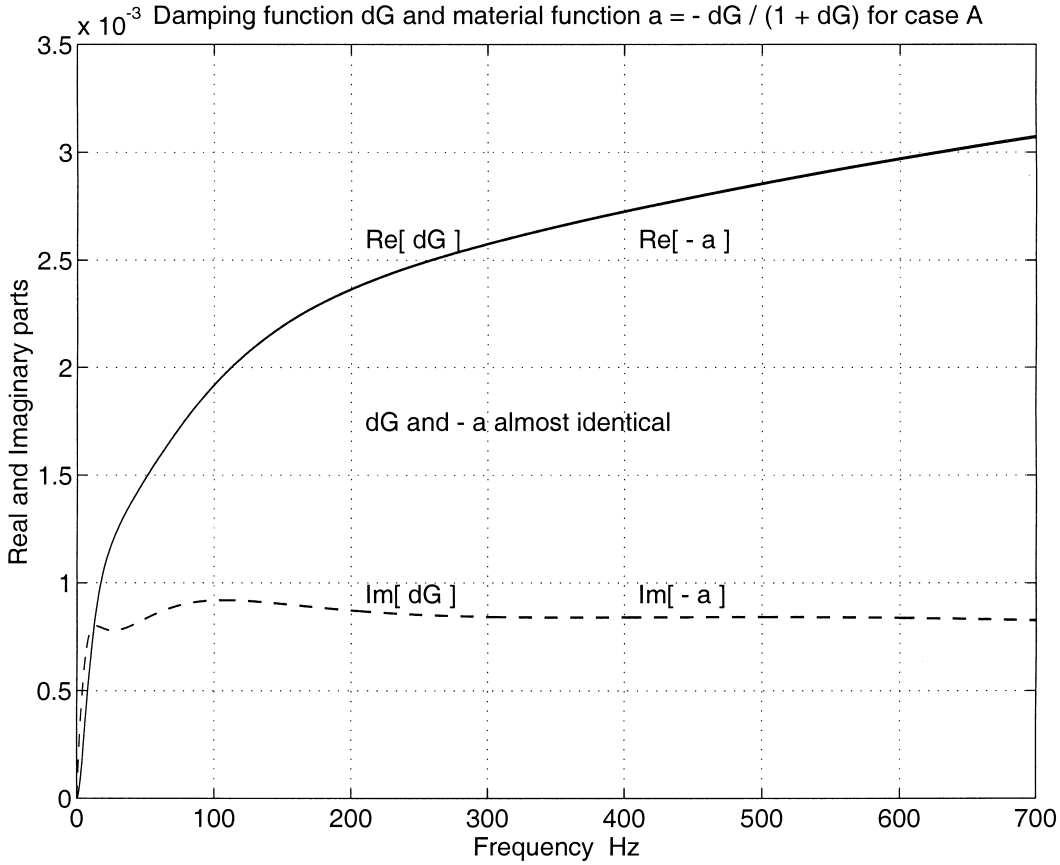

Fig. 2. Isotropic damping function d_G and isotropic material function $a = -d_G/(1 + d_G)$ for case A (Table 1). Real parts (solid line) and imaginary parts (dashed line).

was done using the AHL elements implemented, cf. Dovstam (1997) in ASKA Acoustics, Göransson (1988). All modal simulations were done using MATLAB®.

As numerical test object was chosen the same cantilever, rectangular plate as used for test of the uncoupled, modal receptance model presented in Dovstam (1997). The dimensions (standard SI units are used here) of the test plate were: *thickness* $h = 0.004$ m, *width* $b = 0.070$ m and *length* $L = 0.500$ m. The long straight edges were oriented parallel to the x-axis ($x = x_1$) with the ends at $x = 0$ and $x = L$, respectively, and the displacements were constrained to zero in the yz-plane ($y = x_2$, $z = x_3$) at the fixed end at $x = 0$. The z-axis was oriented orthogonal to the plate faces in the thickness direction.

6.2. Elastic and modal data

The *elastic material parameters* and the *mass density* used for the studied plate were chosen as (estimated for a real polystyrene test piece at room temperature 20°C):

$G = 0.8824 \times 10^9$ Pa
$\lambda = 2.2689 \times 10^9$ Pa
$\rho = 1050$ kg/m^3

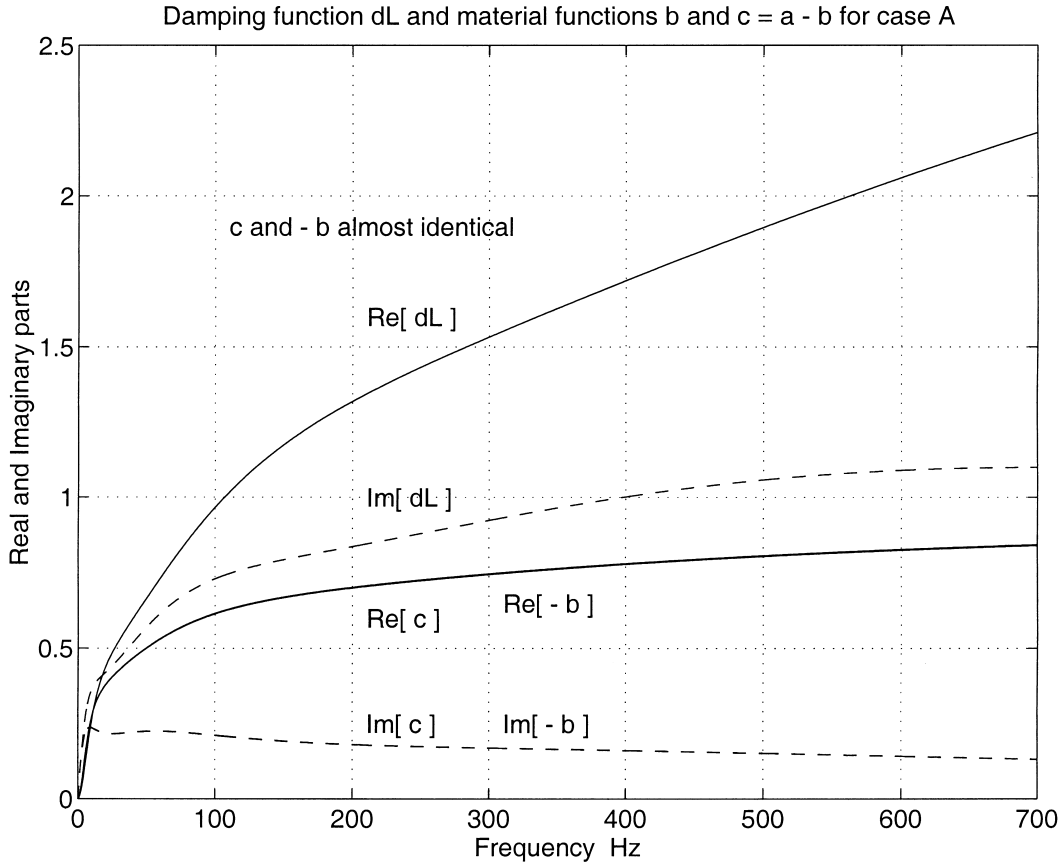

Fig. 3. Isotropic damping function d_λ and isotropic material functions b and $c = a - b$ for case A (Table 1). Real parts (solid line) and imaginary parts (dashed line).

where G and λ correspond to the Young's modulus $E_Y = 2.4 \times 10^9$ Pa and Poisson's ratio $\nu = 0.36$.

In both the direct FE response calculations and in the calculation of FE approximations of the undamped, modal parameters (natural frequencies ω_m, displacement modes $\mathbf{w}^{(m)}(\mathbf{x})$ and partial, isotropic modal strain energy integrals γ_{mr}), the plate was modelled using isoparametric, volume elements (20 nodes per element) with one element through the plate thickness, 14 elements in the y-direction and 100 elements along the x-direction. Thus, a total number of 1400 three-dimensional elements (size: $0.004 \times 0.005 \times 0.005$ m^3), with three displacement degrees of freedom per node.

The *computed modal data* used here are exactly the same as those presented and used in Dovstam (1997). Here, though, the isotropic strain energy integrals, γ_{mr}, are used in a new coupled modal model. The natural frequencies, $f_m = \omega_m/2\pi$, number 1, 16, 100 and 200, taken as examples, were calculated to $f_1 = 3.96$ Hz, $f_{16} = 677$ Hz, $f_{100} = 6642$ Hz and $f_{200} = 12{,}243$ Hz, respectively. Isotropic weight factors χ_m and isotropic coupling matrix elements C_{mr}, cf. Eqs. (62) and (66), were calculated for the 200 lowest modes of the plate. The maximum χ_m-value, corresponding to an almost pure torsional mode, was $\chi_3 = 0.99$ for mode number 3, while the minimum value was $\chi_{58} = 0.85$ for mode number 58. The largest positive and negative coupling matrix elements C_{mr} were $C_{1,\,103} = 15.1$ and $C_{1,\,106} = -47.5$, respectively, for all 200 modes, showing the largest coupling between stress mode coefficients 1 and 106. The

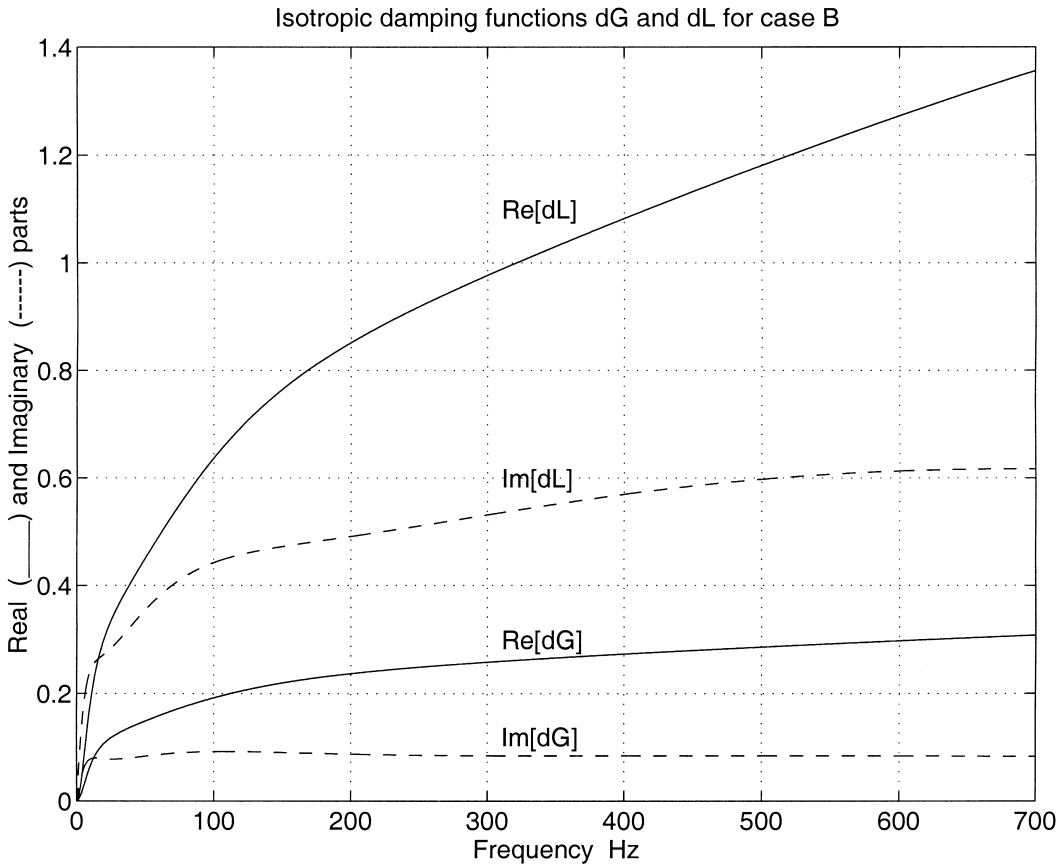

Fig. 4. Isotropic damping functions d_G and d_λ for case B (Table 1). Real parts (solid line) and imaginary parts (dashed line).

maximum and minimum elements in row number 2 of the coupling matrix, representing coupling between mode 2 and the other modes, were $C_{2,\,106} = 6.25$ and $C_{2,\,107} = -5.22$, respectively, showing that also mode number 2 was most strongly coupled to mode 106. All remaining coupling matrix elements, in rows number 3 to 200, were much smaller. The χ_m factors (dots) and the maximum absolute value of the off-diagonal elements (circles) in each row m of the coupling matrix C_{mr}) are shown in Fig. 1.

6.3. Damping and predicted frequency shifts

To simulate homogeneous *isotropic*, non-proportional *damping* in the chosen material, hypothetical damping functions d_λ and d_G were defined by the relations (cf. Dovstam, 1995, 1997, 1998b and Section 3.2):

$$d_G(s) = \sum_{n=1}^{3} \frac{2\mu_n^2}{G\alpha_n} \cdot \frac{s}{(s+\beta_n)} \tag{70}$$

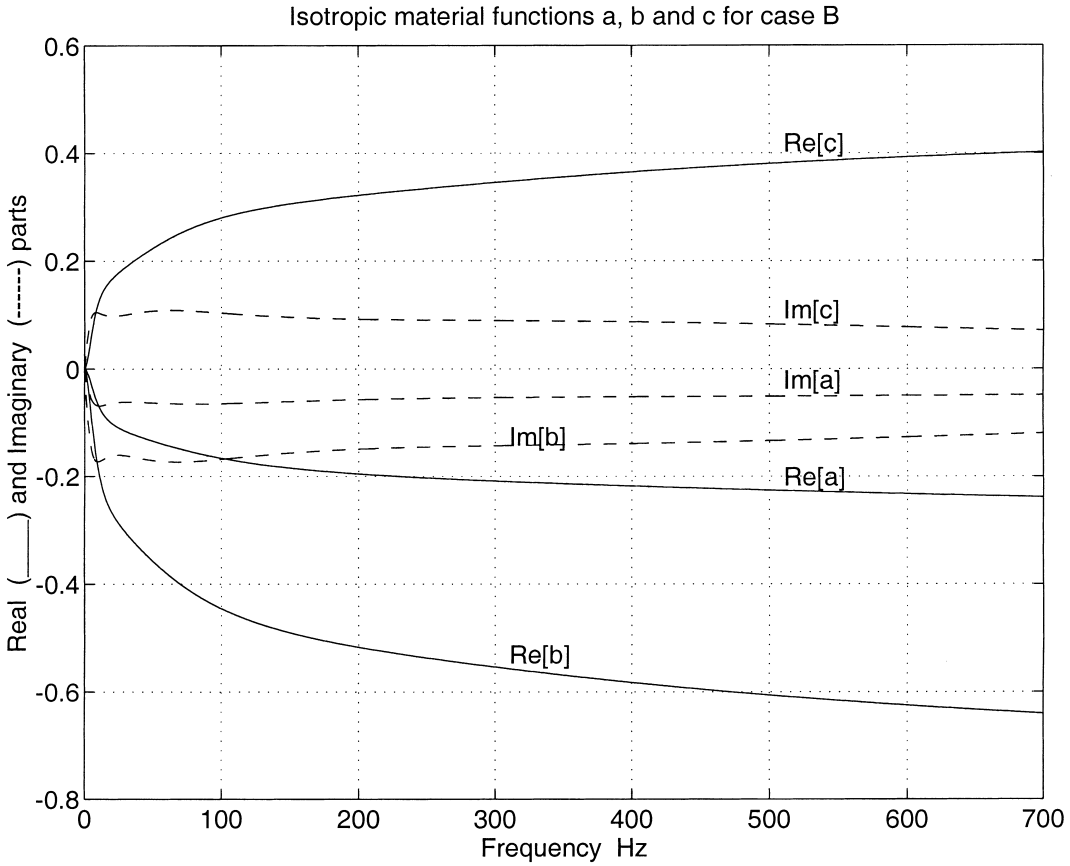

Fig. 5. Isotropic material funtions $a = -d_G/(1 + d_G)$, b and $c = a - b$ for case B (Table 1). Real parts (solid line) and imaginary parts (dashed line).

$$d_\lambda(s) = \sum_{n=1}^{3} \frac{\left(3\varphi_n^2 + 4\varphi_n\mu_n\right)}{\lambda\alpha_n} \cdot \frac{s}{\left(s + \beta_n\right)} \tag{71}$$

using the AHL material damping parameter values β_n, μ_n and φ_n in Table 1. The dissipation parameters α_n were all taken equal to unity (Dovstam, 1997) and the choice of three damping processes with the particular relaxation frequencies β_n in Table 1, was made in order to generate a high enough damping in the frequency range below 700 Hz, where the cantilever test plate has a sufficiently high number of undamped natural frequencies (16 below 700 Hz, cf. Table 2) to be suitable for test of the new modal model.

Three cases, each with different but homogeneous, isotropic material damping, were studied. Two of the cases, cases A and B (Table 1), were also discussed in Dovstam (1997); while the third case, case C (Table 1), is a new case with extremely high damping but, nevertheless, very small modal coupling in the studied frequency range. Common to all three cases is a very high *material* damping level which results in both relatively small (case A) and extremely high (case C) *structural* modal damping.

The different material damping functions $d_G(s)$ and $d_\lambda(s)$ and the corresponding new material

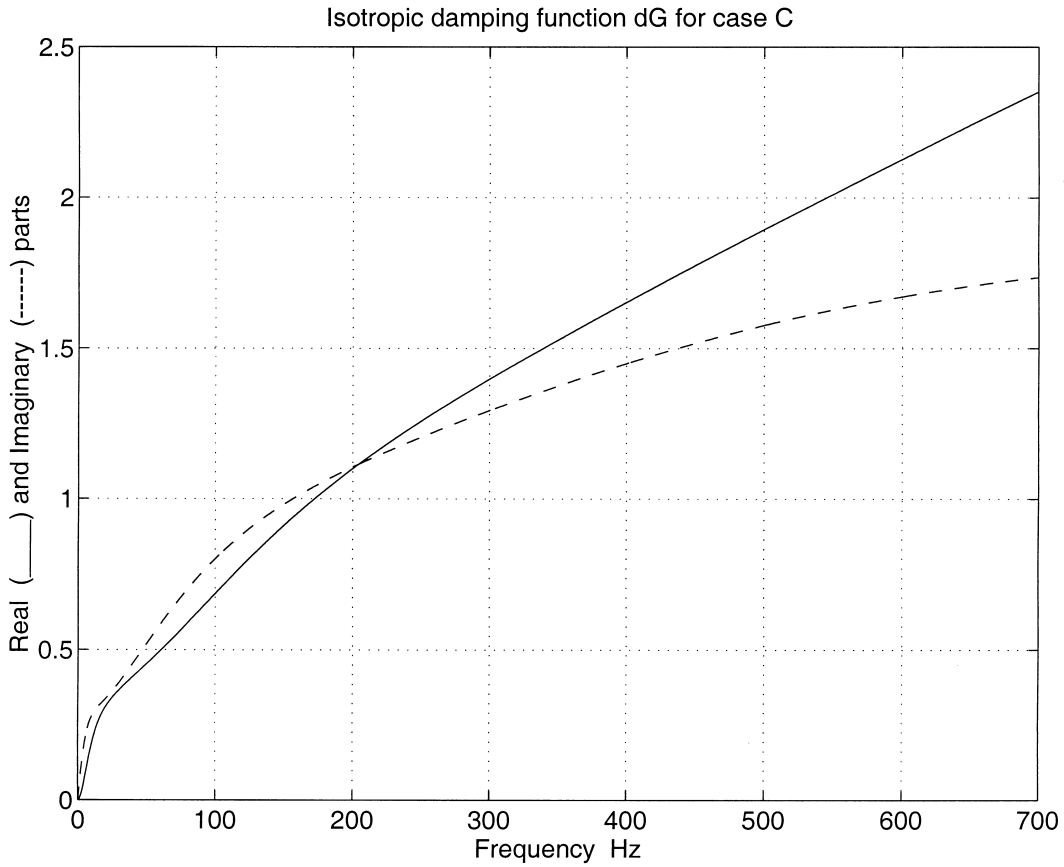

Fig. 6. Isotropic damping function d_G for case C (Table 1). Real part (solid line) and imaginary part (dashed line).

functions $a(s)$, $b(s)$ and $c(s) = a(s) - b(s)$ (cf. Eqs. (56), (57) and (60)) are presented for each case in Figs. 2 and 3 (case A), Figs. 4 and 5 (case B) and Figs. 6 and 7 (case C).

From Fig. 2, it is obvious that $d_G(s)$ and the material function $a(s)$ in case A are very small and could be neglected compared to $d_\lambda(s)$, $b(s)$ and $c(s) = a(s) - b(s)$ presented in Fig. 3. In case B, as can be seen in Figs. 4 and 5, the two damping functions $d_G(s)$ and $d_\lambda(s)$ and all the material functions $a(s)$, $b(s)$ and $c(s) = a(s) - b(s)$ have real and imaginary parts of about the same order of magnitude. Thus, in case B both material functions $a(s)$ and $b(s)$ will contribute to the modal damping in the modal system equations (53), cf. Eqs. (56)–(60). In case C, the damping function $d_\lambda(s)$ is identically zero, while the real and imaginary parts of $d_G(s)$ are very large, Fig. 6. The material function $a(s)$ dominates the contribution to the modal shift functions $\delta_m(s)$ and the system matrix elements $B_{mr}(s)$ in Eq. (58) in case C, Fig. 7. This follows from Eq. (59) and the fact that the modal weights χ_m are all larger than 0.85 for the studied test plate.

It should be noted here that *for vanishing* $d_\lambda(s)$, the isotropic material function $b(s)$ is given by:

$$\left[b(s)\right]_{d_\lambda=0} = -\frac{\left[d_G(s)\right]^2}{1 + 3\lambda/(2G) + \left[2 + 3\lambda/(2G)\right] \cdot d_G(s) + \left[d_G(s)\right]^2} \tag{72}$$

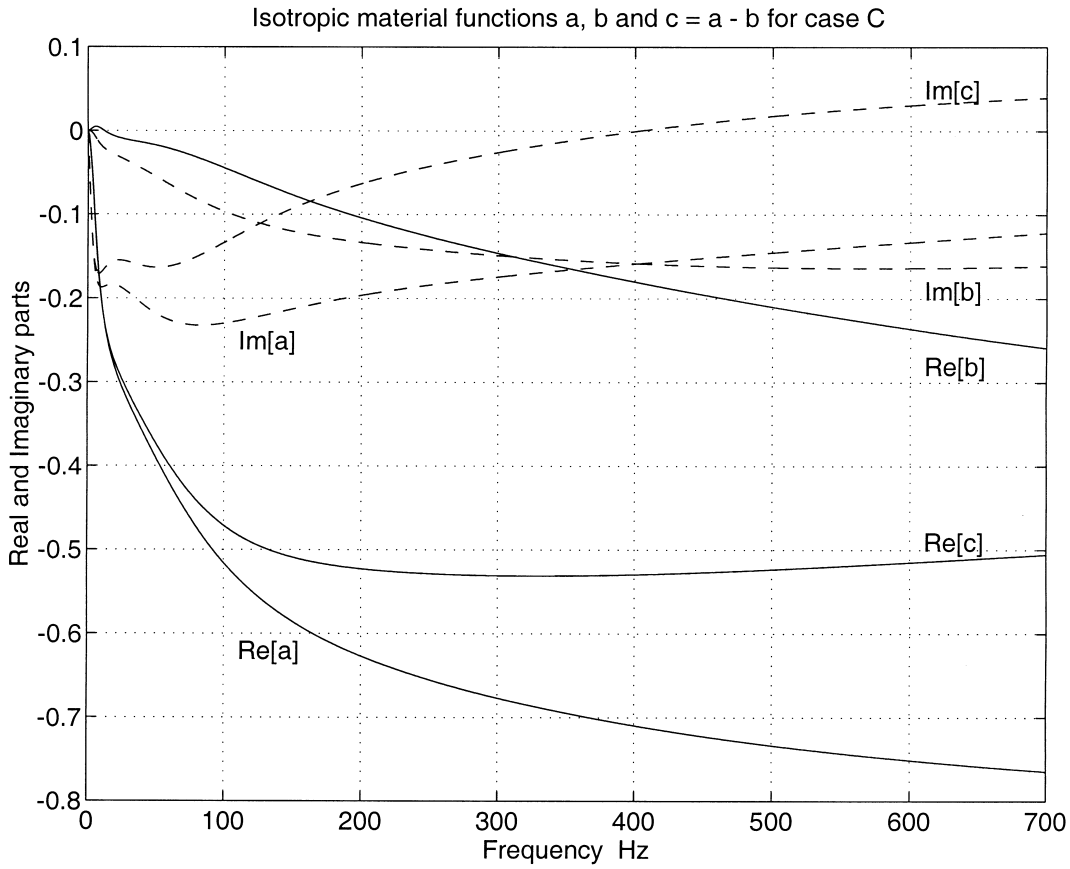

Fig. 7. Isotropic material functions $a = -d_G/(1 + d_G)$, b and $c = a - b$ for case C (Table 1). Real parts (solid line) and imaginary parts (dashed line).

where $3\lambda/2G = 3.86$ for the test plate. Thus, it follows that, for vanishing $d_\lambda(s)$, $b(s)$ may be neglected when d_G is small but not when d_G is large.

Typical modal shift functions $\delta_m(s)$, defined by Eq. (59), are presented in Fig. 8 for case A and three different χ_m-values ($\chi_m = 0.85$, 0.90 and 0.99). In connection to the shift functions, it is interesting to note that $-\mathrm{Im}[\delta_m(i\omega_{md})]$ could be used as a measure of the *structural (modal) damping* for mode number m. From Fig. 8, it is clear that the modal damping in case A should be small, which is also confirmed by the responses (Figs. 9 and 10) calculated for case A.

Modal frequency shifts, predicted using the relationship (63), for the three cases A, B and C are given in Table 2 for modes with predicted damped resonance frequencies below 700 Hz. As can be seen, the frequency shifts in case C are extremely large for all but the two lowest modes. Further, the shifts predicted for case A agree closely with the peaks in the computed displacement responses (cf. Table 2 and the receptance in Figs. 9 and 10). Good agreement between predicted shifts and observed peak frequencies is obtained also in case B, even though the peaks in case B, due to the high modal damping, are "overlapping" and the corresponding frequencies not so easily identified (cf. Table 2 and the receptances in Fig. 11). In case C, no pronounced sharp peaks are observed, Fig. 12, due to very high damping.

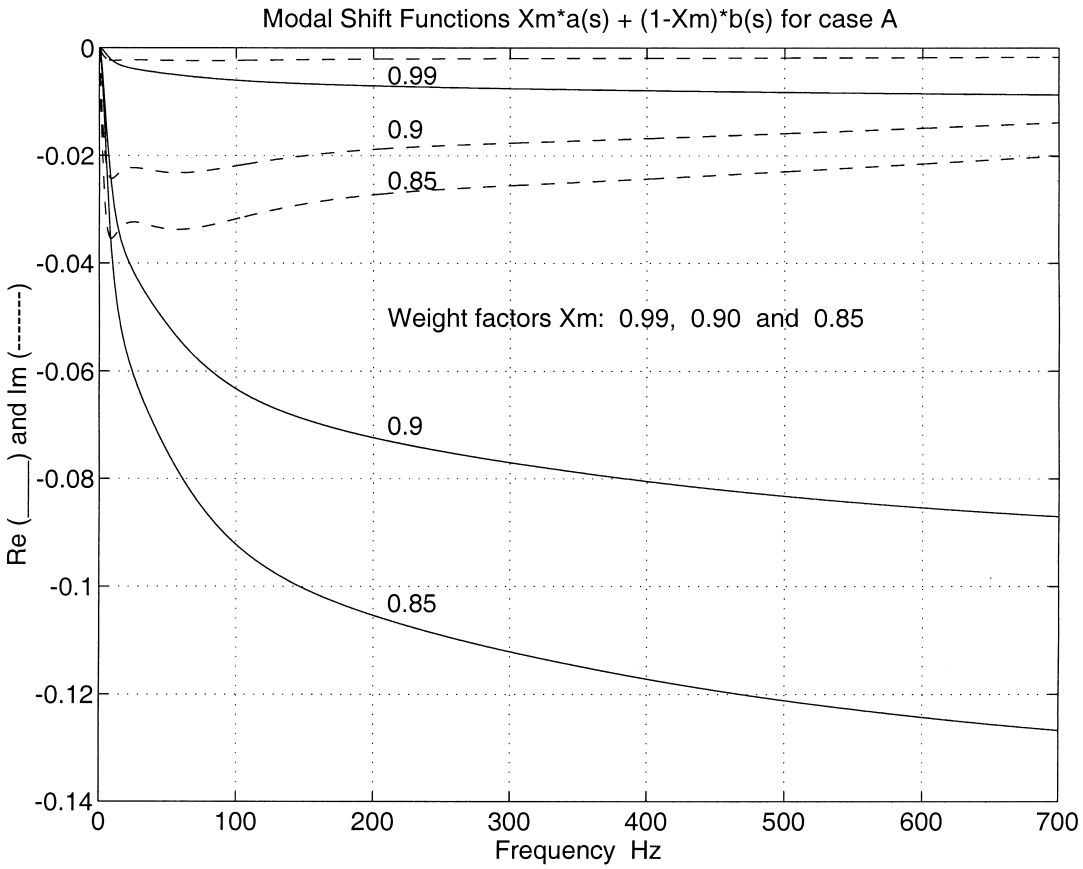

Fig. 8. Modal shift functions $\delta_m = \chi_m \cdot a + (1 - \chi_m) \cdot b$ for case A (Table 1). Modal weight factor values $\chi_m = 0.99$, 0.90 and 0.85. Real parts (solid line) and imaginary parts (dashed line).

6.4. Modal and direct FE response simulations

All modal and direct FE response simulations presented here are magnitude, receptance spectra $|R_{3F_3}|$ (Section 2) corresponding to a dynamic (idealised) point force with *unit spectrum* $\tilde{F}_z = \tilde{F}_3 = 1$ and $\tilde{F}_1 = \tilde{F}_2 = 0$) in the z-direction at the *excitation point* $x_e = L$, $y_e = b$, $z_e = h$. As a consequence of the idealised point force used as excitation, the calculated direct FE responses correspond to a larger number of excited modes than in the modal simulation which has to be truncated after a number, N, of modes, cf. Eq. (3). This has to be taken into account when comparing results from direct FE and modal simulations, especially when comparing responses at the excitation point.

Responses in the z-direction at the excitation point and at the *opposite corner* $x = L$, $y = 0$, $z = h$ are presented for case A. For cases B and C, the response at the opposite free corner is presented.

Direct FE responses were computed in the frequency range 200–700 Hz with frequency resolution $\Delta f = 2.51$ Hz, while the modal response simulations were computed using frequency resolution $\Delta f = 1$ Hz and a number of $N = 100$ modes. Computed and used displacement modes were visually inspected, and judged to be good approximations of the corresponding, unknown but desired, continuous, elastic normal modes.

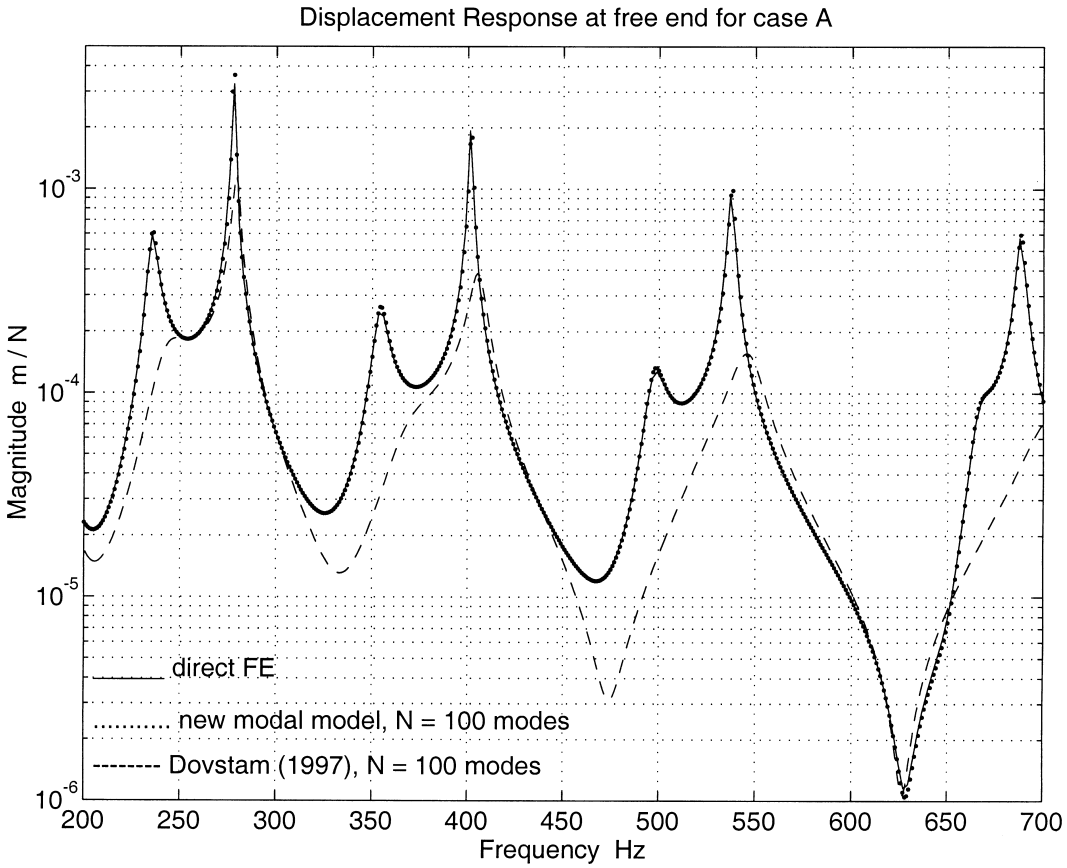

Fig. 9. Absolute value of receptance $R_{33} = R_{3F}$ for case A (Table 1). Response in $z = x_3$-direction in upper corner at free end due to force excitation in same direction in the opposite upper corner at the free end. *Solid* line, response computed using direct FE. *Dotted* line, response calculated, using the new correctly coupled modal model, according to Eqs. (2), (3), (46), (53) and (58). *Dashed* line, modal response, calculated using the uncoupled model in Dovstam (1997). All modal calculations with $N = 100$ modes and modal forces $\tilde{F}_\partial^{(m)} = w_3^{(m)}(\mathbf{x}_e)$. Frequency range 200–700 Hz.

The responses calculated for case A are presented in Fig. 9 (response at free corner) and Fig. 10 (response at excitation point), while the response (at free corner) in case B is presented in Fig. 11. The highly damped response in case C is presented in Fig. 12 (response at free corner).

As already mentioned, cases A and B were also studied in Dovstam (1997), where the old uncoupled receptance model, though, showed bad convergence for case B and very bad for case A. For all cases A, B and C, modal simulations using the old uncoupled modal receptance model are shown here, for reference, as dashed lines in Figs. 9–12.

The simulations using the new, unconditionally, convergent modal technique (using Eqs. (2), (3), (30), (46), (53) and (55)–(62)) agree extremely well with corresponding direct FE calculations (solid, thin line in the diagrams) in all cases A, B and C, as can be seen in Figs. 9–12. Some minor differences can be seen in Fig. 10 in the vicinity of the deep valleys at about 460, 510 and 615 Hz. These differences, though, are attributed to the modal truncation at $N = 100$ modes and the point force excitation in the

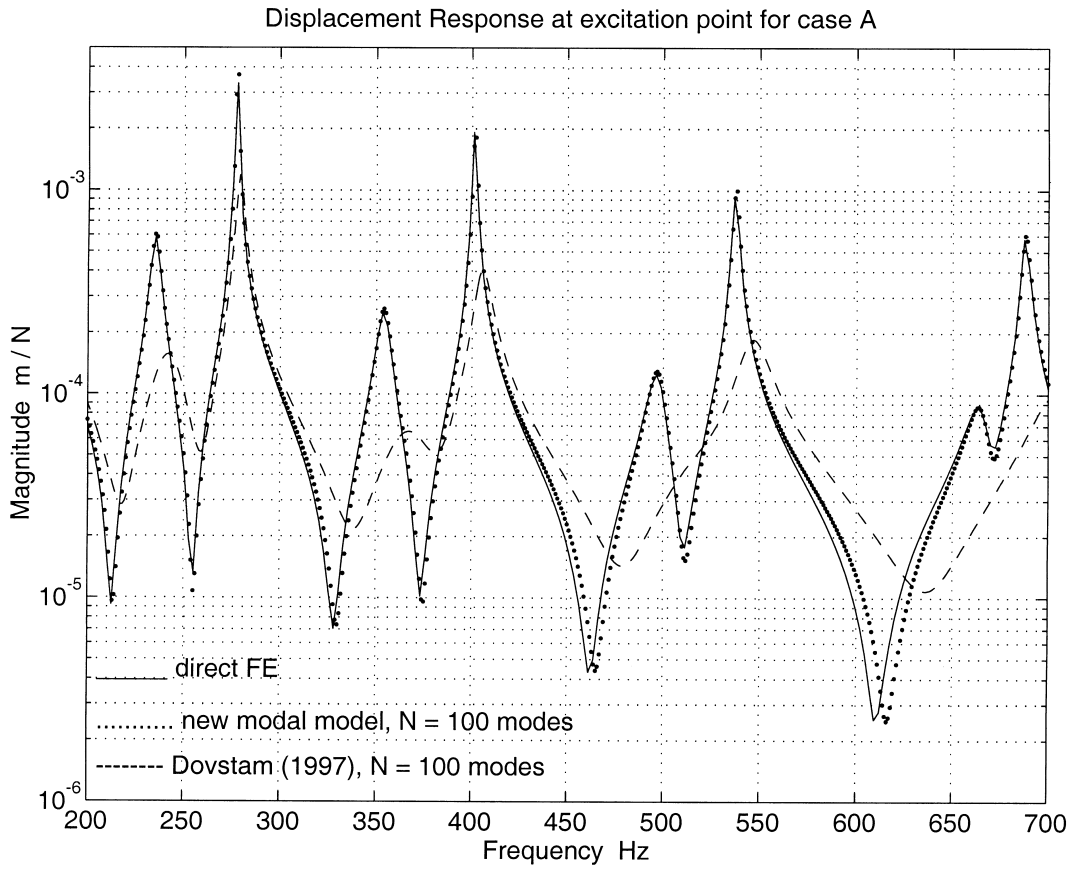

Fig. 10. Absolute value of receptance $R_{33} = R_{3F}$ for case A (Table 1). Response in $z = x_3$-direction at the excitation point in upper corner at free end. *Solid* line, response computed using direct FE. *Dotted* line, response calculated, using the new correctly coupled modal model, according to Eqs. (2), (3), (46), (53) and (58). *Dashed* line, modal response, calculated using the uncoupled model in Dovstam (1997). All modal calculations with $N = 100$ modes and modal forces $\tilde{F}_{\vartheta}^{(m)} = w_3^{(m)}(\mathbf{x}_e)$. Frequency range 200–700 Hz.

modal model while using consistent force excitation and (of course) no corresponding truncation in the direct FE calculations.

Uncoupled modal responses have also been computed using the approximation (67), valid for small stress mode coupling. For the same number of modes, this uncoupled modal model results in the same response as the fully coupled modal model with the exception for the response presented in Fig. 12 (at free corner in case C). As can be seen in Fig. 12, neither the old uncoupled model (Dovstam, 1997) nor the new uncoupled model (67) agree completely with the calculated direct FE response. Thus, Fig. 12 indicates that there is some modal coupling present in case C, for the studied frequencies, which has to be taken into account to get good agreement between the direct FE and modal simulations.

Finally, as evident from the presented Figs. 9–12, the frequency shifts due to the damping, discussed in Sections 5.3 and 6.3 above, are predicted extremely well by the new modal technique in all cases A, B and C.

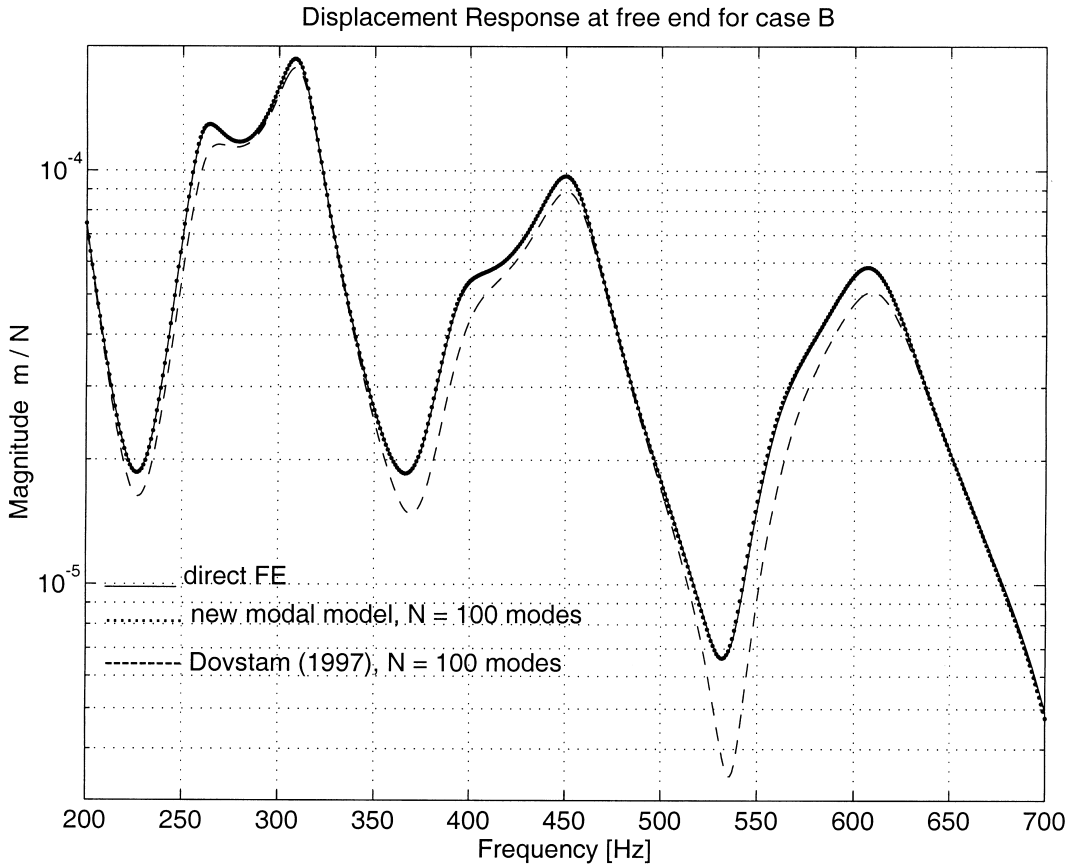

Fig. 11. Absolute value of receptance $R_{33} = R_{3F}$ for case B (Table 1). Response in $z = x_3$-direction in upper corner at free end due to force excitation in same direction in the opposite upper corner at the free end. *Solid* line, response computed using direct FE. *Dotted* line, response calculated, using the new correctly coupled modal model, according to Eqs. (2), (3), (46), (53) and (58). *Dashed* line, modal response, calculated using the uncoupled model in Dovstam (1997). All modal calculations with $N = 100$ modes and modal forces $\tilde{F}_\partial^{(m)} = w_3^{(m)}(\mathbf{x}_e)$. Frequency range 200–700 Hz.

7. Summary

An unconditionally convergent method for modal expansion of vibrational displacement fields in linear, but otherwise generally damped, continuous bodies and structures is proposed. The method and the corresponding modal response model is based on continuous displacement modes and implicit use of continuous, dual stress modes.

The new results are needed and crucial in cases where the different matrix elements of the anelastic part $\mathbf{H}_\Delta$ in the AHL, $\hat{\mathbf{H}} = \mathbf{H} + \mathbf{H}_\Delta$, have different frequency dependence; while they, at the same time, cannot be considered as small compared to corresponding elasticities in the generalised Hooke's law material matrix field $\mathbf{H}$.

The real eigenvalue problem defining the continuous, elastic stress modes, equivalent and dual to classical, continuous, normal displacement modes used in traditional modal expansion, is formulated; and frequency domain modal (system) equations of motion for computation of needed generalised

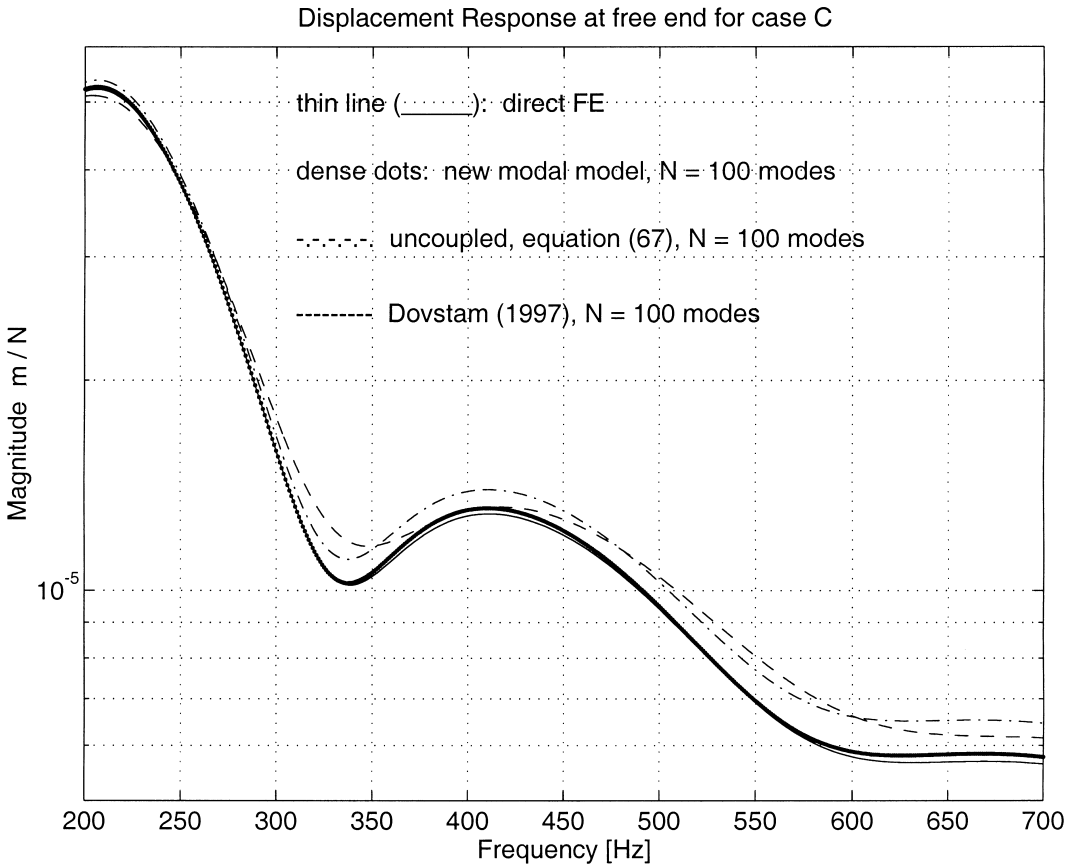

Fig. 12. Absolute value of receptance $R_{33} = R_{3F}$ for case C (Table 1). Response in $z = x_3$-direction in upper corner at free end due to force excitation in same direction in the opposite upper corner at the free end. *Solid* line, response computed using direct FE. *Dotted* line, response calculated, using the new correctly coupled modal model, according to Eqs. (2), (3), (46), (53) and (58). *Dashed* line, modal response, calculated using the uncoupled model in Dovstam (1997). *Dashed-dotted* line, modal response calculated using Eq. (67), neglecting modal cross coupling, and thus assuming small stress mode coupling. All modal calculations with $N = 100$ modes and modal forces $\tilde{F}_\partial^{(m)} = w_3^{(m)}(\mathbf{x}_e)$. Frequency range 200–700 Hz.

Fourier coefficient functionals (stress and displacement mode coefficient spectra) are derived for cases with boundary traction excitation.

Introduced modal coupling parameters are computable from known material properties (elastic moduli, damping and mass distribution) and geometry by post processing results from three-dimensional, standard FE (displacement) eigenvalue calculations.

When the damping and coupling approach zero, the new method approaches the uncoupled modal model discussed in Dovstam (1997).

The results are explicitly applied to the case with homogeneous, isotropic damping, and means are provided for predicting damped resonance frequencies and for predicting whether coupling will occur or not.

The method is verified on the numerical test cases presented in Dovstam (1997), which showed poor or very bad convergence for the uncoupled modal receptance model. The agreement between direct FE

calculations and response simulations using the new modal method is extremely good in all cases studied.

The proposed modal response model makes it possible to separate elastic and geometry dependent modal properties from the dissipation and damping properties of a vibrating solid or structure which is very important in experimental damping estimation based on response measurements (Dovstam, 1997; Dovstam and Dalenbring, 1997).

The new theory provides also an improved theoretical basis for experimental modal analysis (Ewins, 1986) and refinement of hybrid modal analysis (Dovstam, 1998a).

Acknowledgements

This work was performed under contract from the Swedish Defence Material Administration (Contract No. 23250-93-102-24-001). The funding provided is gratefully acknowledged.

Many thanks to Peter Göransson, Stella Einarsson and Mats Dalenbring (all at FFA Acoustics and Structural Dynamics department) and Adam Zdunek (FFA Strength of material department) for valuable discussions and criticism.

Thanks also to Mats Dalenbring for doing the necessary FE modelling and computations in ASKA Acoustics.

Appendix A. Definitions

The Cartesian matrix representations **u**, **T** and **E** of the displacement field, the symmetric stress and (infinitesimal) strain tensor fields, respectively, are defined as:

$$\mathbf{u} = \mathbf{u}(\mathbf{x}, t) = \begin{bmatrix} u_1 & u_2 & u_3 \end{bmatrix}^{\mathrm{T}} \tag{A1}$$

$$\mathbf{T} = \mathbf{T}(\mathbf{x}, t) = \begin{bmatrix} \sigma_{11} & \sigma_{22} & \sigma_{33} & \sigma_{12} & \sigma_{23} & \sigma_{31} \end{bmatrix}^{\mathrm{T}} \tag{A2}$$

$$\mathbf{E} = \mathbf{E}(\mathbf{x}, t) = \begin{bmatrix} \varepsilon_{11} & \varepsilon_{22} & \varepsilon_{33} & 2\varepsilon_{12} & 2\varepsilon_{23} & 2\varepsilon_{31} \end{bmatrix}^{\mathrm{T}} \tag{A3}$$

where u_i, σ_{ik} and ε_{ik} are Cartesian vector and tensor components. Likewise the matrix representations of the modal displacement field number m and the stress mode field number m, respectively, are defined as:

$$\mathbf{w}^{(m)} = \mathbf{w}^{(m)}(\mathbf{x}) = \begin{bmatrix} w_1^{(m)} & w_2^{(m)} & w_3^{(m)} \end{bmatrix}^{\mathrm{T}} \tag{A4}$$

$$\mathbf{S}^{(m)} = \mathbf{S}^{(m)}(\mathbf{x}) = \begin{bmatrix} \sigma_{11}^{(m)} & \sigma_{22}^{(m)} & \sigma_{33}^{(m)} & \sigma_{12}^{(m)} & \sigma_{23}^{(m)} & \sigma_{31}^{(m)} \end{bmatrix}^{\mathrm{T}} \tag{A5}$$

The current infinitesimal strains ε_{ik} and the infinitesimal modal strains $\varepsilon_{ik}^{(m)}$ are defined, respectively, as:

$$\varepsilon_{ik} = \frac{1}{2}\left[\frac{\partial u_i}{\partial x_k} + \frac{\partial u_k}{\partial x_i}\right] \tag{A6}$$

$$\varepsilon_{ik}^{(m)} = \frac{1}{2}\left[\frac{\partial w_i^{(m)}}{\partial x_k} + \frac{\partial w_k^{(m)}}{\partial x_i}\right] \tag{A7}$$

The strain vectors $\mathbf{E}$ and $\mathbf{E}^{(m)}$, corresponding to those strains, may be determined from the matrix fields $\mathbf{u}$ and $\mathbf{w}^{(m)}$ as:

$$\mathbf{E} = \mathbf{D}[\mathbf{u}] \tag{A8}$$

$$\mathbf{E}^{(m)} = \mathbf{D}\left[\mathbf{w}^{(m)}\right] \tag{A9}$$

where the first order, partial differential operator matrix $\mathbf{D}$ is the Cartesian 6×3-matrix representation:

$$\mathbf{D} = \mathbf{D}[\ ] = \begin{bmatrix} \frac{\partial}{\partial x_1} & 0 & 0 & \frac{\partial}{\partial x_2} & 0 & \frac{\partial}{\partial x_3} \\ 0 & \frac{\partial}{\partial x_2} & 0 & \frac{\partial}{\partial x_1} & \frac{\partial}{\partial x_3} & 0 \\ 0 & 0 & \frac{\partial}{\partial x_3} & 0 & \frac{\partial}{\partial x_2} & \frac{\partial}{\partial x_1} \end{bmatrix}^{\mathrm{T}} \tag{A10}$$

of the three-dimensional, spatial, symmetric gradient operator (Gurtin, 1972).

The Cartesian matrix representation $\mathbf{N} = \mathbf{N}(\mathbf{x})$ of the unit normal vector field $\mathbf{n} = \mathbf{n}(\mathbf{x})$ is defined as:

$$\mathbf{N} = \begin{bmatrix} n_1 & 0 & 0 & n_2 & 0 & n_3 \\ 0 & n_2 & 0 & n_1 & n_3 & 0 \\ 0 & 0 & n_3 & 0 & n_2 & n_1 \end{bmatrix} \tag{A11}$$

Cartesian traction vector components $(\mathbf{t}_\mathrm{n})_k$ are defined by unit normal components n_i and symmetric, Cartesian stress tensor components σ_{ik} as:

$$(\mathbf{t}_\mathrm{n})_k = \sigma_{ik} n_i \quad \text{sum on } i \tag{A12}$$

which in matrix form is equivalent to:

$$\mathbf{t}_\mathrm{n} = \mathbf{NT} \tag{A13}$$

The only *non-zero* elements of the real 6×6 matrices $\mathbf{H}_\lambda$ and $\mathbf{H}_G$ in the isotropic, elastic generalised Hooke's law matrix $\mathbf{H} = \lambda\mathbf{H}_\lambda + G\mathbf{H}_G$ are:

$$(\mathbf{H}_\lambda)_{ik} = 1 \quad i, k \le 3 \tag{A14}$$

$$(\mathbf{H}_G)_{ii} = 2, \qquad 1 \le i \le 3;\ (\mathbf{H}_G)_{ii} = 1, \quad 4 \le i \le 6 \tag{A15}$$

Appendix B. Inner products and $L_2(\Omega)$ convergence

The $\mathbf{L}_2^3(\Omega) \equiv L_2(\Omega) \times L_2(\Omega) \times L_2(\Omega)$ inner product $(\mathbf{u}, \mathbf{v})$ is defined (Oden, 1979) as:

$$(\mathbf{u}, \mathbf{v}) = \int_\Omega \mathbf{u} \cdot \mathbf{v}^* \, \mathrm{d}\Omega = \int_\Omega \left(u_1 v_1^* + u_2 v_2^* + u_3 v_3^*\right) \mathrm{d}\Omega \tag{B1}$$

where $\mathbf{v}^*$ denotes the complex conjugate of the complex (having complex valued component fields), three-dimensional vector field $\mathbf{v}$. The natural norm in $\mathbf{L}_2^3(\Omega)$, induced by the inner product $(\mathbf{u}, \mathbf{v})$, is defined as:

$$\|\tilde{\mathbf{u}}\| = \sqrt{(\tilde{\mathbf{u}}, \tilde{\mathbf{u}})} \tag{B2}$$

for the complex vector field $\tilde{\mathbf{u}}$.

A sequence $\{\mathbf{u}_n\}_{n=1}^{\infty}$ converges to $\mathbf{u}$ in the sense of the $\mathbf{L}_2^3(\Omega)$ norm if (cf. Mikhlin, 1964; Gurtin, 1972; Oden, 1979):

$$\lim_{n\to\infty} \|\mathbf{u} - \mathbf{u}_n\| = \lim_{n\to\infty} \sqrt{(\mathbf{u} - \mathbf{u}_n, \mathbf{u} - \mathbf{u}_n)} = 0 \tag{B3}$$

The inner product $(\mathbf{u}, \mathbf{v})_\partial$ for vector fields on the boundary $\partial\Omega$ is defined as:

$$(\mathbf{u}, \mathbf{v})_\partial = \int_{\partial\Omega} \mathbf{u} \cdot \mathbf{v}^* \, \mathrm{d}\partial\Omega \tag{B4}$$

Analogously, the $\mathbf{L}_2^6(\Omega) \equiv \mathbf{L}_2^3(\Omega) \times \mathbf{L}_2^3(\Omega)$ inner product $\langle \mathbf{E}, \mathbf{V} \rangle$ of two six-dimensional vector fields $\mathbf{E}$ and $\mathbf{V}$ is defined as:

$$\langle \mathbf{E}, \mathbf{V} \rangle = \int_\Omega \left(E_1 V_1^* + E_2 V_2^* + \cdots + E_6 V_6^* \right) \mathrm{d}\Omega \tag{B5}$$

Here, $\mathbf{V}^*$ denotes the complex conjugate of the vector field $\mathbf{V}$. All stress and strain vector fields discussed are assumed to belong to $\mathbf{L}_2^6(\Omega)$.

For arbitrary three- and six-dimensional fields $\mathbf{v}$ and $\mathbf{A}$, it may be shown by partial integration (Gauss' theorem) that:

$$\left(\mathbf{D}^{\mathrm{T}}[\mathbf{A}], \mathbf{v}\right) + \langle \mathbf{A}, \mathbf{D}[\mathbf{v}] \rangle = (\mathbf{N}\mathbf{A}, \mathbf{v})_\partial \tag{B6}$$

$$\langle \mathbf{D}[\mathbf{v}], \mathbf{A} \rangle + \left(\mathbf{v}, \mathbf{D}^{\mathrm{T}}[\mathbf{A}]\right) = (\mathbf{v}, \mathbf{N}\mathbf{A})_\partial \tag{B7}$$

In particular, it may be derived for the operator $\hat{\mathbf{L}}$ that:

$$\left(\hat{\mathbf{L}}[\tilde{\mathbf{u}}], \mathbf{v}\right) = \langle \hat{\mathbf{H}}\mathbf{D}[\tilde{\mathbf{u}}], \mathbf{D}[\mathbf{v}] \rangle - \left(\mathbf{N}\hat{\mathbf{H}}\mathbf{D}[\tilde{\mathbf{u}}], \mathbf{v}\right)_\partial \tag{B8}$$

and for the "elastic" operator $\mathbf{L}$ ($\mathbf{L}_a$ is the adjoint of $\mathbf{L}$):

$$(\mathbf{L}[\mathbf{u}], \mathbf{v}) = \langle \mathbf{H}\mathbf{D}[\mathbf{u}], \mathbf{D}[\mathbf{v}] \rangle - (\mathbf{N}\mathbf{H}\mathbf{D}[\mathbf{u}], \mathbf{v})_\partial \tag{B9}$$

$$(\mathbf{L}[\mathbf{u}], \mathbf{v}) = (\mathbf{u}, \mathbf{L}_a[\mathbf{v}]) + (\mathbf{u}, \mathbf{N}\mathbf{H}\mathbf{D}[\mathbf{v}])_\partial - (\mathbf{N}\mathbf{H}\mathbf{D}[\mathbf{u}], \mathbf{v})_\partial \tag{B10}$$

where $\mathbf{u}$ and $\mathbf{v}$ are arbitrary, complex, three-dimensional vector fields in $\mathbf{L}_2^3(\Omega)$. The adjoint $\mathbf{L}_a$ is formally defined as:

$$\mathbf{L}_a[\mathbf{v}] = -\mathbf{D}^{\mathrm{T}}[\mathbf{H}\mathbf{D}[\mathbf{v}]] = \mathbf{L}[\mathbf{v}] \tag{B11}$$

Due to a well known property of Hilbert spaces (related to termwise integration, see e.g. Reddy, 1986)

$$\langle \tilde{\mathbf{T}}_N, \mathbf{X} \rangle \to \langle \tilde{\mathbf{T}}, \mathbf{X} \rangle \tag{B12}$$

for any $\mathbf{X}$ in $\mathbf{L}_2^6(\Omega)$ if $\tilde{\mathbf{T}}_N \rightarrow \tilde{\mathbf{T}}$ in $\mathbf{L}_2^6(\Omega)$. This important fact is utilised in the modal expansion of anelastic strain contributions.

Appendix C. Convergence of $\tilde{\mathbf{T}}_N$ in $\mathbf{L}_2^6(\Omega)$

Utilising the orthogonality properties (44) for dual, **u**-compatible modes, it follows from Eqs. (33), (46) and (B12) that:

$$\langle \tilde{\mathbf{T}}_N, \mathbf{C}\tilde{\mathbf{T}}_N \rangle = \sum_{m=1}^{N} \frac{1}{a_m \omega_m^2} |\tilde{F}_\partial^{(m)} - s^2 a_m c_m(\tilde{\mathbf{u}})|^2 \leq \sum_{m=1}^{N} \frac{1}{\omega_m^2} \left\{ \frac{1}{a_m} |\tilde{F}_\partial^{(m)}|^2 + |s|^4 \cdot a_m |c_m(\tilde{\mathbf{u}})|^2 + 2|s|^2 \cdot |\tilde{F}_\partial^{(m)}||c_m(\tilde{\mathbf{u}})| \right\} \tag{C1}$$

Now, due to Parseval's theorem for discrete complex Hilbert spaces ℓ^2 (cf. e.g. Oden, 1979), it may be shown that $\sum_{m=1}^{\infty} |\tilde{F}_\partial^{(m)}||c_m(\tilde{\mathbf{u}})|$ is finite if the infinite sums $\sum_{m=1}^{\infty} \frac{1}{a_m} |\frac{\tilde{F}_\partial^{(m)}}{\omega_m}|^2$ and $\sum_{m=1}^{\infty} a_m |\frac{c_m(\tilde{\mathbf{u}})}{\omega_m}|^2$ both are finite. It follows thus from Eq. (C1), when $\tilde{\mathbf{u}}_N$ converges to $\tilde{\mathbf{u}}$ in $\mathbf{L}_2^3(\Omega)$ (which it always does, due to completeness of the displacement modes $\mathbf{w}^{(m)}$), that $\tilde{\mathbf{T}}_N$ converges to $\tilde{\mathbf{T}}$ in the *energy norm* $\|\cdot\|_{\mathrm{C}}$:

$$\langle \tilde{\mathbf{T}}_N, \mathbf{C}\tilde{\mathbf{T}}_N \rangle \rightarrow \langle \tilde{\mathbf{T}}, \mathbf{C}\tilde{\mathbf{T}} \rangle = \|\tilde{\mathbf{T}}\|_{\mathrm{C}} \tag{C2}$$

when N goes to infinity *if* the infinite sum $\sum_{m=1}^{\infty} \frac{1}{a_m} |\frac{\tilde{F}_\partial^{(m)}}{\omega_m}|^2$ is bounded. In practice, $|\tilde{F}_\partial^{(m)}|$ may be neglected for m larger than some $m_{\max}$ (due to short spatial wave lengths of all modes $\mathbf{w}^{(m)}$ with high enough mode number m combined with locally distributed but spatially smooth excitation). The sums in Eq. (C1) with terms containing $\tilde{F}_\partial^{(m)}$ are, therefore, finite and bounded, and $\tilde{\mathbf{T}}_N$ converges thus, in practice, to $\tilde{\mathbf{T}}$ *in energy* as defined by Eq. (C2).

The elastic compliance matrix field, $\mathbf{C} = \mathbf{H}^{-1}$, is further assumed to be *bounded below* (cf. the *ellipticity conditions* of linear elasticity, Oden, 1979) and there exists, therefore, a real positive constant α_{C} such that for all $\mathbf{X}$ in $\mathbf{L}_2^6(\Omega)$:

$$\|\mathbf{X}\|_{\mathrm{C}} = \sqrt{\langle \mathbf{X}, \mathbf{C}\mathbf{X} \rangle} \geq \alpha_{\mathrm{C}} \cdot \|\mathbf{X}\|_{\mathbf{L}_2^6(\Omega)} \tag{C3}$$

where the norm in $\mathbf{L}_2^6(\Omega)$ is $\|\cdot\|_{\mathbf{L}_2^6(\Omega)} = \sqrt{\langle \cdot, \cdot \rangle}$. It thus follows that:

$$\|\tilde{\mathbf{T}}_N\|_{\mathbf{L}_2^6(\Omega)} \leq \frac{1}{\alpha_{\mathrm{C}}} \cdot \|\tilde{\mathbf{T}}_N\|_{\mathrm{C}} = \frac{1}{\alpha_{\mathrm{C}}} \sqrt{\langle \tilde{\mathbf{T}}_N, \mathbf{C}\tilde{\mathbf{T}}_N \rangle} \tag{C4}$$

As a consequence, in all realistic applications, the modal, stress series approximation converges to the correct $\tilde{\mathbf{T}}$ in $\mathbf{L}_2^6(\Omega)$ when $\tilde{\mathbf{u}}_N$ converges to $\tilde{\mathbf{u}}$ in $\mathbf{L}_2^3(\Omega)$.

Appendix D. Dual elastic modes

By definition, an *elastic stress mode* $\mathbf{S}^{(m)}$ is the solution to the eigenvalue problem:

$$\mathbf{Q}[\mathbf{S}^{(m)}] = \bar{\omega}_m^2 \cdot \mathbf{C}\mathbf{S}^{(m)} \tag{D1}$$

$$\left(\rho^{-1}\mathbf{D}^{\mathrm{T}}\left[\mathbf{S}^{(m)}\right], \mathbf{N}\mathbf{S}^{(r)}\right)_{\partial} = 0 \tag{D2}$$

where $\bar{\omega}_m$ is the circular eigenfrequency of mode number m.

Analogously, for an *elastic displacement mode* $\mathbf{w}^{(m)}$ with corresponding circular eigenfrequency ω_m and elastic (generalised Hooke) material matrix $\mathbf{H} = \mathbf{C}^{-1}$, the following equivalent relationships can be written down (cf. the definitions of the second-order operators $\mathbf{L}$ and $\mathbf{Q}$ in the main text, Eqs. (32) and (16), respectively):

$$\mathbf{L}\left[\mathbf{w}^{(m)}\right] = \omega_m^2 \cdot \rho\mathbf{w}^{(m)} \tag{D3}$$

$$-\mathbf{D}^{\mathrm{T}}\mathbf{H}\mathbf{D}\left[\mathbf{w}^{(m)}\right] = \omega_m^2 \cdot \rho\mathbf{w}^{(m)} \tag{D4}$$

$$-\mathbf{D}\left\{\rho^{-1}\mathbf{D}^{\mathrm{T}}\mathbf{H}\mathbf{D}\left[\mathbf{w}^{(m)}\right]\right\} = \omega_m^2 \cdot \mathbf{D}\left[\mathbf{w}^{(m)}\right] \tag{D5}$$

$$\mathbf{Q}[\mathbf{H}\mathbf{E}^{(m)}] = \omega_m^2 \cdot \mathbf{E}^{(m)} \tag{D6}$$

and, due to the assumption $\mathbf{C} = \mathbf{H}^{-1}$, from Eq. (D6)

$$\mathbf{Q}[\mathbf{H}\mathbf{E}^{(m)}] = \omega_m^2 \cdot \mathbf{C}\mathbf{H}\mathbf{E}^{(m)} \tag{D7}$$

According to Eq. (D1), it follows from Eq. (D7) that $\bar{\mathbf{S}}^{(m)} \equiv \mathbf{H}\mathbf{E}^{(m)}$ is a *stress mode with the same eigenvalue* ω_m^2 *as the displacement mode* $\mathbf{w}^{(m)}$. Due to Eq. (D4) and the boundary conditions (26) in the main text, it follows finally that

$$\left(\mathbf{N}\mathbf{H}\mathbf{E}^{(r)}, \mathbf{w}^{(m)}\right)_{\partial} = -\omega_m^{-2} \cdot \left(\mathbf{N}\bar{\mathbf{S}}^{(r)}, \rho^{-1}\mathbf{D}^{\mathrm{T}}\left[\bar{\mathbf{S}}^{(m)}\right]\right)_{\partial} = 0 \quad \text{all } r, m \tag{D8}$$

Thus, the modes $\mathbf{w}^{(m)}$ and $\bar{\mathbf{S}}^{(m)} \equiv \mathbf{H}\mathbf{E}^{(m)} \equiv \mathbf{H}\mathbf{D}[\mathbf{w}^{(m)}]$ not only correspond to the same positive eigenvalue ω_m^2 but also satisfy equivalent boundary conditions (26) and (D2).

Alternatively, starting with Eq. (D1), the equivalent relationships are obtained:

$$\mathbf{H}\mathbf{Q}\left[\mathbf{S}^{(m)}\right] = \bar{\omega}_m^2 \cdot \mathbf{S}^{(m)} \tag{D9}$$

$$-\mathbf{H}\mathbf{D}\left[\rho^{-1}\mathbf{D}^{\mathrm{T}}\left[\mathbf{S}^{(m)}\right]\right] = \bar{\omega}_m^2 \cdot \mathbf{S}^{(m)} \tag{D10}$$

$$-\mathbf{D}^{\mathrm{T}}\mathbf{H}\mathbf{D}\left[\rho^{-1}\mathbf{D}^{\mathrm{T}}\left[\mathbf{S}^{(m)}\right]\right] = \bar{\omega}_m^2 \cdot \mathbf{D}^{\mathrm{T}}\left[\mathbf{S}^{(m)}\right] \tag{D11}$$

which are all equivalent to Eq. (D1). After introduction of the displacement fields

$$\mathbf{v}^{(m)} \equiv \rho^{-1}\mathbf{D}^{\mathrm{T}}\left[\mathbf{S}^{(m)}\right] \tag{D12}$$

it follows from Eq. (D11) and the definition of $\mathbf{L}$, (32), that

$$\mathbf{L}\left[\mathbf{v}^{(m)}\right] = \bar{\omega}_m^2 \cdot \rho\mathbf{v}^{(m)} \tag{D13}$$

According to Eq. (31), in the main text, and Eq. (D13), it is thus clear that $\mathbf{v}^{(m)} \equiv \rho^{-1}\mathbf{D}^{\mathrm{T}}[\mathbf{S}^{(m)}]$ is a *displacement mode with the same eigenvalue* $\bar{\omega}_m^2$ *as the stress mode* $\mathbf{S}^{(m)}$. Further, due to Eqs. (D10) and

(D12) and the boundary conditions (37), it follows that:

$$\left(\mathbf{NS}^{(r)},\, \rho^{-1}\mathbf{D}^{\mathrm{T}}\left[\mathbf{S}^{(m)}\right]\right)_{\partial} = -\bar{\omega}_r^{-2}\cdot\left(\mathbf{NHD}\left[\mathbf{v}^{(r)}\right],\, \mathbf{v}^{(m)}\right]\right)_{\partial} = 0 \quad \text{all } r,\, m \tag{D14}$$

Thus, the fields $\mathbf{v}^{(m)}$ and $\mathbf{S}^{(m)}$ correspond to the same positive eigenvalue $\bar{\omega}_m^2$ and satisfy equivalent boundary conditions (37) and (D14).

The fields $\mathbf{v}^{(m)}$ are of course related to the displacement modes $\mathbf{w}^{(m)}$. Comparing Eq. (D4) and the definition (D12), it follows, thus, that the displacement mode $\mathbf{w}^{(m)}$ is related to the stress mode $\mathbf{S}^{(m)}$ as:

$$\mathbf{w}^{(m)} = -\omega_m^{-2}\rho^{-1}\mathbf{D}^{\mathrm{T}}\left[\mathbf{S}^{(m)}\right] \tag{D15}$$

which is equivalent to the relation:

$$\mathbf{S}^{(m)} = \mathbf{HE}^{(m)} = \mathbf{HD}\left[\mathbf{w}^{(m)}\right] \tag{D16}$$

Due to the duality relations (D15) and (D16), the mode sets $\mathbf{w}^{(m)}$ and $\mathbf{S}^{(m)}$ are in the present paper denoted *dual* (elastic) *modes*.

From Eq. (B9) and the assumption $\mathbf{C} = \mathbf{H}^{-1}$, it follows finally, for $\mathbf{S}^{(r)} = \mathbf{HE}^{(r)}$ and $\mathbf{S}^{(m)} = \mathbf{HE}^{(m)}$ that:

$$\begin{aligned}\langle \mathbf{S}^{(m)},\, \mathbf{CS}^{(r)}\rangle &= \langle \mathbf{S}^{(m)},\, \mathbf{CHE}^{(r)}\rangle = \langle \mathbf{S}^{(m)},\, \mathbf{E}^{(r)}\rangle = \langle \mathbf{HE}^{(m)},\, \mathbf{E}^{(r)}\rangle \\ &= \left(\mathbf{L}\left[\mathbf{w}^{(m)}\right],\, \mathbf{w}^{(r)}\right) + \left(\mathbf{NHE}^{(m)},\, \mathbf{w}^{(r)}\right)_{\partial} = \omega_m^2\cdot\left(\rho\mathbf{w}^{(m)},\, \mathbf{w}^{(r)}\right) + \left(\mathbf{t}_{\mathrm{n}}^{(m)},\, \mathbf{w}^{(r)}\right)_{\partial}\end{aligned} \tag{D17}$$

After applying the boundary conditions (26) in the main text

$$\langle \mathbf{S}^{(m)},\, \mathbf{CS}^{(r)}\rangle = \langle \mathbf{HE}^{(m)},\, \mathbf{E}^{(r)}\rangle = a_m\cdot\omega_m^2\cdot\delta_{mr} = L_m\cdot\delta_{mr} \tag{D18}$$

and it follows for dual stress and displacement modes that:

$$L_m = a_m\cdot\omega_m^2 \tag{D19}$$

References

Dalenbring, M., 1999. Damping function estimation based on measured vibration frequency responses and finite-element displacement modes. J. Mechanical Systems and Signal Processing 13, 547–569.

Dovstam, K., 1995. Augmented Hooke's law in frequency domain. A three-dimensional, material damping formulation. Int. J. Solids Structures 32, 2835–2852.

Dovstam, K., 1997. Receptance model based on isotropic damping functions and elastic displacement modes. Int. J. Solids Structures 34, 2733–2754.

Dovstam, K., Dalenbring, M., 1997. Damping function estimation based on modal receptance models and neural nets. Computational Mechanics 19 (4), 271–286.

Dovstam, K., 1998a. Real modes of vibration and hybrid modal analysis. Computational Mechanics 21 (6), 493–511.

Dovstam, K., 1998b. On material damping modelling and modal analysis in structural dynamics. Ph.D. Thesis, Department of Solid Mechanics, Royal Institute of Technology, Stockholm, Sweden.

Dovstam, K., 1999. Augmented Hooke's law based on alternative stress relaxation models. To be submitted.

Ewins, D.J., 1986. Modal Testing: Theory and Practice. Research Studies Press Ltd., Letchworth, England and Brüel & Kjaer, Naeram, Denmark.

Gurtin, M.E., 1972. The linear theory of elasticity. In: Flügge, S., Truesdell, C. (Eds.), Encyclopedia of Physics, Volume VIa/2, Mechanics of Solids II. Springer, Berlin.

Göransson, P., 1988. ASKA Acoustics. Theory and Applications. In: FFA TN 1988-13. The Aeronautical Research Institute of Sweden, Stockholm.

Ignaczak, J., 1963. A completeness problem for stress equations of motion in the linear elasticity theory. Archivum Mechaniki Stosowdnej 15 (2), 225–234.

Mikhlin, S.G., 1964. Variational Methods in Mathematical Physics. Pergamon Press, Oxford.

Oden, J.T., 1979. Applied Functional Analysis. Prentice-Hall, Englewood Cliffs, NJ.

Reddy, J.N., 1986. Applied Functional Analysis and Variational Methods in Engineering. McGraw-Hill, New York.